Title:
Toxicokinetic studies of the four new psychoactive substances 4-chloroethcathinone, N-ethylnorpentylone, N-ethylhexedrone, and 4-fluoro-alpha-pyrrolidinohexiophenone

Authors:
Lea Wagmann, Sascha K. Manier, Niels Eckstein, Hans H. Maurer & Markus R. Meyer

This is a post-peer-review, pre-copyedit version of an article published in *Forensic Toxicology* (Volume 38, Pages 59–69(2020), DOI: 10.1007/s11419-019-00487-w)
The final authenticated version is available online at: https://doi.org/10.1007/s11419-019-00487-w

Toxicokinetic studies of the four new psychoactive substances 4-chloroethcathinone, *N*-ethylnorpentylone, *N*-ethylhexedrone, and 4-fluoro-alpha-pyrrolidinohexiophenone

Lea Wagmann[a], Sascha K. Manier[a], Niels Eckstein[b], Hans H. Maurer[a], Markus R. Meyer[a]

[a] Department of Experimental and Clinical Toxicology, Institute of Experimental and Clinical Pharmacology and Toxicology, Center for Molecular Signaling (PZMS), Saarland University, Homburg, Germany

[b] Department of Applied Pharmacy, University of Applied Sciences Kaiserslautern, Campus Pirmasens, Pirmasens, Germany

Contact

Markus R. Meyer, Department of Experimental and Clinical Toxicology, Institute of Experimental and Clinical Pharmacology and Toxicology, Center for Molecular Signaling (PZMS), Saarland University, Homburg, Germany

E-mail: markus.meyer@uks.eu

ABSTRACT

Purpose

The presented study aimed to elucidate the toxicokinetics of the four synthetic cathinones 4-chloroethcathinone (4-CEC), *N*-ethylnorpentylone (*N*-ethylpentylone, ephylone), *N*-ethylhexedrone (NEH), and 4-fluoro-alpha-pyrrolidinohexiophenone (4-fluoro-alpha-pyrrolidinohexanophenone, 4-F-α-PHP, 4F-alpha-PHP, 4F-PHP).

Methods

First, their metabolism was studied using human urine and blood samples. Analysis of specimens was performed by liquid chromatography-high resolution tandem mass spectrometry (LC-HRMS/MS) and gas chromatography-mass spectrometry (GC-MS). LC-HRMS/MS was also used to analyze in vitro incubations of the new psychoactive substances using pooled human liver S9 fraction (pS9), to identify the monooxygenases involved in the initial metabolic steps, and determination of plasma concentrations after standard addition method. Metabolic stability was tested in pooled human liver microsomes incubations analyzed by LC-ion trap MS.

Results

Using LC-HRMS/MS, in total 47 metabolites were found in patient samples and pS9 incubations. Using GC-MS, 4-CEC, ephylone, NEH, and five of their metabolites were detectable in urine. The following main phase I reactions were observed: carbonyl group reduction, *N*-deethylation, hydroxylation, lactam formation (4F-PHP), and demethylenation (ephylone). Mainly glucuronidations were observed as phase II reactions besides conjugates with the dicarboxylic acids malonic, succinic, and glutaric acid (4-CEC), sulfation, methylation (both ephylone), and *N*-acetylation (NEH). A broad range of monooxygenases was involved in the initial steps with exception of NEH (only CYP1A2 and CYP2C19). 4F-PHP had the shortest in vitro half-life (38 min) and highest intrinsic clearance (15.7 $mL \times min^{-1} \times kg^{-1}$). Plasma concentrations ranged from 0.8 to 8.5 ng/mL.

Conclusions

Our results are expected to help toxicologists to reliably identify these substances in case of

suspected abuse and allow them a thorough risk assessment.

KEY WORDS

Drugs of abuse, NPS, novel psychoactive substances, metabolism study, toxicokinetics, screening targets

Introduction

The global new psychoactive substances (NPS) market is still characterized by the emergence of large numbers of new substances belonging to diverse chemical groups. Synthetic cathinones represent one of the largest groups and are frequently reported to the United Nations Office on Drugs and Crime (UNODC) [1]. Synthetic cathinones are chemically related to cathinone, which is a naturally occurring stimulant found in the khat plant (*Catha edulis*), and their pharmacodynamic profile is similar to that of other psychomotor stimulants including amphetamine-like monoamine releasing properties or cocaine-like blockade of monoamine reuptake [2, 3]. As most synthetic cathinones are sold as "legal highs" and not internationally controlled, they represent an ongoing issue for clinical and forensic toxicologists who must identify an unending variety of new drugs of abuse [4]. The knowledge about the toxicokinetics of NPS is essential for analytics but also for thorough risk assessment particularly if compounds are co-ingested with other NPS and/or therapeutics. In terms of cathinone abuse, the parent compound is often detectable in human specimens including urine [3], but identification of metabolites may confirm a positive screening result or allow a detection in late excretion phases.

The current study was based on specimens collected from a 41-year-old male who was admitted to the hospital displaying uncontrolled movements and aggressive behavior. The toxicological screening detected four synthetic cathinones (see Figure 1), by name 4-chloroethcathinone (4-CEC), *N*-ethylnorpentylone (*N*-ethylpentylone, ephylone), *N*-ethylhexedrone (NEH), and 4-fluoro-alpha-pyrrolidinohexiophenone (4-fluoro-alpha-pyrrolidinohexanophenone, 4-F-α-PHP, 4F-alpha-PHP, 4F-PHP) in blood and urine samples. The patient was discharged from hospital the next day due to an uneventful course. No metabolites of the detected NPS were described yet, with exception of four ephylone phase I metabolites detected in incubations with human liver microsomes (HLM) [5]. The rationale and aim of the present study was therefore to identify metabolites in patient specimens using liquid chromatography coupled to high-resolution tandem mass spectrometry (LC-HRMS/MS) and gas chromatography-mass spectrometry (GC-MS). Metabolites should be confirmed by and compared to in vitro incubations of the identified NPS

using pooled human liver S9 fraction (pS9). Based on these data suitable analytical targets should be recommended. The monooxygenases involved in the initial metabolic steps should be identified, plasma concentrations determined, and a metabolic stability study in pooled HLM (pHLM) conducted to expand the knowledge surrounding these synthetic cathinones' toxicokinetics.

Materials and methods

Chemicals and enzymes

4-CEC, ephylone, NEH, and 4F-PHP were obtained from an online vendor of NPS based in the Netherlands and identity as well as purity confirmed by HPLC, IR, and MS/MS. Stock solutions of the synthetic cathinones were prepared in methanol (1 mg/mL, each) and stored at -20°C until use. Trimipramine-d_3 was from LGC (Wesel, Germany), $NADP^+$ from Biomol (Hamburg, Germany), isocitrate, isocitrate dehydrogenase, superoxide dismutase, 3′-phosphoadenosine-5′-phosphosulfate (PAPS), *S*-(5′-adenosyl)-L-methionine (SAM), dithiothreitol (DTT), reduced glutathione (GSH), acetyl coenzyme A (AcCoA), magnesium chloride ($MgCl_2$), potassium dihydrogenphosphate, dipotassium hydrogenphosphate, and Tris hydrochloride from Sigma-Aldrich (Taufkirchen, Germany). Zinc sulfate heptahydrate, acetonitrile (LC-MS grade), ammonium formate (analytical grade), formic acid (LC-MS grade), methanol (LC-MS grade), and all other chemicals and reagents (analytical grade) were obtained from VWR (Darmstadt, Germany). The baculovirus-infected insect cell microsomes (Supersomes) containing 1 nmol/mL of human cDNA-expressed CYP1A2, CYP2A6, CYP2B6, CYP2C8, CYP2C9 (2 nmol/mL), CYP2C19, CYP2D6, CYP2E1 (2 nmol/mL), CYP3A4, CYP3A5 (2 nmol/mL), or FMO3 (5 mg protein/mL), and pHLM (20 mg microsomal protein/mL, 360 pmol total CYP/mg protein, 26 individual donors), pS9 (20 mg microsomal protein/mL, 25 individual donors), UGT reaction mixture solution A (25 mM UDP-glucuronic acid), and UGT reaction mixture solution B (250 mM Tris HCl, 40 mM $MgCl_2$, and 125 µg/mL alamethicin) were obtained from Corning (Amsterdam, The Netherlands). After delivery, the

enzyme preparations were thawed at 37°C, aliquoted, snap-frozen in liquid nitrogen, and stored at −80°C until use.

Preparation of human biosamples

Authentic heparinized human blood plasma and human urine samples after suggested intake of drugs of abuse were submitted for clinical toxicological analysis to the authors' laboratory. The blood sample was centrifuged and plasma was separated. Plasma and urine were kept frozen (−20°C) until analysis. Human plasma (250 µL) was prepared according to Helfer et al. by precipitation with 750 µL of a zinc sulfate solution (35 mg/mL in water:methanol, 70:30, *v/v*) [6]. After shaking and centrifugation (18,407 x g, 2 min), the supernatant was transferred into an LC vial and injected onto the LC-HRMS/MS system. Human urine (100 µL) was prepared according to Wissenbach et al. by precipitation with 500 µL of acetonitrile [7]. After shaking and centrifugation (18,407 x g, 2 min), the supernatant was transferred into a glass vial and evaporated to dryness under a gentle stream of nitrogen at 50°C. The residue was dissolved in 50 µL of a mixture of eluent A and B (for LC-HRMS/MS, see chapter 2.7, 1:1, *v/v*), transferred into an LC vial, and injected onto the LC-HRMS/MS system. For analysis by GC-MS, the authors' standard liquid-liquid extraction for plasma and systematic toxicological analysis procedure for urine, consisting of hydrolysis, extraction, and microwave-assisted acetylation was used, and GC-MS standard operation conditions [8]. Briefly, a Hewlett Packard (HP, Agilent Technologies, Waldbronn, Germany) 5890 Series II gas chromatograph, an HP 5970 MSD mass spectrometer, a cross-linked methylsilicone capillary Optima-5 MS (12 m×0.2 mm I.D.), film thickness 0.35 µm (Macherey-Nagel, Düren, Germany) and the following conditions were used: injector port temperature, 280 °C; carrier gas, helium; flow rate 1 ml/min; column temperature, programmed from 100 to 310 °C at 30°/min, initial time 3 min, final time 5 min; electron ionization (EI) mode, ionization energy, 70 eV; ion source temperature, 200 °C; and scan rate, 1 scan/sec.

In vitro incubations for metabolism studies

As previously described by Richter et al. [9], the final incubation volume was 150 µL. Incubations were performed using pS9 (2 mg microsomal protein/mL) after preincubation for 10 min at 37 °C with 25 µg/mL alamethicin (UGT reaction mixture solution B), 90 mM phosphate buffer (pH 7.4), 2.5 mM Mg^{2+}, 2.5 mM isocitrate, 0.6 mM $NADP^{+}$, 0.8 U/mL isocitrate dehydrogenase, 100 U/mL superoxide dismutase, and 0.1 mM AcCoA. Thereafter, 2.5 mM UDP-glucuronic acid (UGT reaction mixture solution A), 40 µM PAPS, 1.2 mM SAM, 1 mM DTT, 10 mM GSH, and 25 µM substrate (one of the four synthetic cathinones) were added. All given concentrations correspond to the final concentrations in one reaction tube. The organic solvent content in the final incubation mixtures was always below 1% [10]. The reaction was initiated by addition of the substrate and the reaction mixture was incubated for a maximum of 360 min. After 60 min, an aliquot of 60 µL of the incubation mixture was transferred to a reaction tube containing 20 µL ice-cold acetonitrile for termination of the reactions. The remaining mixture was incubated for additional 300 min and thereafter stopped by addition of 30 µL ice-cold acetonitrile. After addition of acetonitrile, mixtures were cooled for 30 min at -20°C, centrifuged (18,407 x g, 2 min), and supernatants transferred into LC vials, followed by injection onto the LC-HRMS/MS system. Blank samples without substrate and control samples without pS9 were prepared to confirm the absence of interfering compounds and identification of compounds not formed by metabolism, respectively. All incubations were performed in duplicate (n = 2).

Monooxygenases activity screening

According to a published procedure [11], microsomal incubations in duplicate were performed at 37 °C for 30 min using a substrate concentration of 25 µM and CYP1A2, CYP2A6, CYP2B6, CYP2C8, CYP2C9, CYP2C19, CYP2D6, CYP2E1, CYP3A4, CYP3A5 (75 pmol/mL each), or FMO3 (0.25 mg protein/mL). Reference incubations with pHLM (1 mg microsomal protein/mL) were used as positive control. Control samples without enzymes were prepared to assess formation of compounds not originated from metabolism. Besides enzymes and substrates, the incubation mixtures (final volume, 50 µL) contained 90 mM phosphate buffer (pH 7.4), 5 mM Mg^{2+}, 5 mM

isocitrate, 1.2 mM $NADP^+$, 0.5 U/mL isocitrate dehydrogenase, and 200 U/mL superoxide dismutase. For incubations with CYP2A6 or CYP2C9, phosphate buffer was replaced with 90 mM Tris buffer, respectively, according to the manufacturer's recommendation. Reactions were initiated by addition of the enzyme preparation and terminated by addition of 50 µL of ice-cold acetonitrile. Mixtures were centrifuged (18,407 x g, 2 min), supernatants transferred into LC vials, and injected onto the LC-HRMS/MS system.

Determination of plasma concentrations

Standard addition method was used for quantification of 4-CEC, ephylone, NEH, and 4F-PHP in the authentic human plasma sample. Briefly, 50 µL blood plasma were precipitated with 100 µL acetonitrile containing 0.1% formic acid. Additionally, five samples were prepared using acetonitrile containing the four synthetic cathinones resulting in final plasma concentrations of 2, 4, 6, 8, and 10 µg/L, respectively. Ten µL of trimipramine-d_3 in methanol (2 µg/L final plasma concentration) were added as internal standard. After shaking and centrifugation (-10°C, 21,130 x g, 30 min), the supernatant was transferred into an LC vial and injected onto the LC-HRMS/MS system. For quantification, the ratios of the corresponding peak area of analyte and internal standard in the HR full scan were used.

Metabolic stability studies

Metabolic stability incubations were performed with pHLM in accordance to chapter 2.4 with the following variations: 2.5 µM substrate concentrations were used and incubations stopped after 0, 30, 60, 90, 120, 150, and 180 min (4-CEC, ephylone, NEH) or 0, 15, 30, 45, 60, 75, and 90 min (4F-PHP) incubation time by addition of 50 µL of ice-cold acetonitrile containing 1 µM trimipramine-d_3 as internal standard. Additionally, control incubations (n = 2) without pHLM were prepared to assess degradation of parent compounds not originated from metabolism and stopped after 180 min (4-CEC, ephylone, NEH) or 90 min (4F-PHP). All incubations were performed in duplicate. Mixtures were centrifuged (18,407 x g, 2 min), supernatants transferred into LC vials,

and injected onto the LC-ion trap (IT) MS system. The natural logarithm of the ratios of the corresponding peak area of analyte and internal standard in the HR full scan were used to assess degradation of parent compounds. GraphPad Prism 5.00 (GraphPad Software, San Diego, USA) was used for statistical evaluation. A t-test was used to determine whether ln[peak area ratio]$_{initial}$ values were significantly different from ln[peak area ratio] values in control incubations without pHLM using the following settings: unpaired; two-tailed; significance level, 0.05; confidence intervals, 99%.

According to Baranczewski et al. [12], the following equations were used for calculations:

(1) $\ln[\text{peak area ratio}]_{remaining} = \ln[\text{peak area ratio}]_{initial} - k \times t$ and $t_{1/2} = \frac{\ln(2)}{k}$

(2) $CL_{int,\ micr} = \frac{\ln(2)}{t_{1/2}(min)} \times \frac{[V]_{incubation}(mL)}{[P]_{incubation}(mg)}$

(3) $CL_{int} = CL_{int,\ micr}\ (\frac{mL}{min\ x\ mg}) \times \frac{[Liver](g)}{[BW]\ (kg)} \times SF\ (\frac{mg}{g})$

with k = slope of the linear regression fit, $t_{1/2}$ = in vitro half-life, $CL_{int,\ micr}$ = microsomal intrinsic clearance, CL_{int} = intrinsic clearance, $[V]_{incubation}$ = incubation volume = 0.05, $[P]_{incubation}$ = microsomal protein amount in the incubation = 0.05, $\frac{[Liver]}{[BW]}$ = liver weight normalized by body weight [13] = 26, and SF = scaling factor microsomal protein per gram of liver [12] = 33.

LC-HRMS/MS conditions

A Thermo Fisher Scientific (TF, Dreieich, Germany) Dionex UltiMate 3000 Rapid Separation (RS) UHPLC system with a quaternary UltiMate 3000 RS pump and an HTC PAL autosampler was used and controlled by the Aria MX software. The chromatographic system was coupled to a TF Q-Exactive Focus equipped with a heated electrospray ionization II (HESI-II) source. Injection volume was 10 µL for all samples. LC and MS conditions were in accordance to Michely et al. [14] with minor modifications. Gradient elution was performed using a TF Accucore PhenylHexyl column (100 mm x 2.1 mm inner diameter, 2.6 µm particle size) at 35°C. The mobile phases consisted of 2 mM aqueous ammonium formate containing formic acid (0.1%, *v/v*, pH 3, eluent A)

and 2 mM ammonium formate in acetonitrile/methanol (50:50, *v/v*) containing formic acid (0.1%, *v/v*) and water (1%, *v/v*, eluent B). The gradient was programmed as follows: 0—1 min 1% B, 1—10 min to 99% B, 10—11.5 min hold 99% B, and 11.5—13.5 min hold 1% B, at a flow rate of 0.5 mL/min from 0 to 10 min and 0.8 mL/min from 10 to 13.5 min. The HESI-II source conditions were as follows: heater temperature, 320°C; ion transfer capillary temperature, 320°C; sheath gas, 60 arbitrary units (AU); auxiliary gas, 40 AU; spray voltage, 4.00 kV, and S-lens RF level, 50.0. Mass spectrometric analysis was performed in positive full scan mode and subsequent data-dependent acquisition (DDA) with priority to mass-to-charge ratios (*m/z*) of parent compounds and their expected metabolites (separate inclusion lists for 4-CEC, ephylone, NEH, and 4F-PHP). Discovery mode was chosen to ensure the recording of MS^2 spectra of precursor ions not in the inclusion list. The settings for full scan data acquisition were as follows: polarity, positive; resolution, 35,000; scan range, *m/z* 100—500; automatic gain control (AGC) target, 1e6; maximum injection time (IT), 120 ms; microscans, 1; spectrum data type, profile. The settings for the DDA mode were as follows: dd-MS^2, discovery; resolution, 17,500; isolation window, 1.0 *m/z*; AGC target, 2e5; maximum IT, 250 ms; high collision dissociation cell with stepped normalized collision energy, 17.5, 35.0, 52.5; loop count, 3; minimum AGC target, 2.5e3 (corresponds to a signal intensity threshold of 1.0e4); exclude isotopes, on; and spectrum data type, profile. Mass calibration was performed prior to analysis according to the manufacturer's recommendations using external mass calibration. TF Xcalibur Qual Browser 4.0 software was used for data handling. The settings for automated peak integration were as follows: peak detection algorithm, ICIS; baseline window, 40; area noise factor, 5; and peak noise factor, 10.

LC-ITMS conditions

A TF LXQ linear ion trap mass spectrometer equipped with a HESI-II source and coupled to a TF Accela ultra HPLC (UHPLC) system consisting of a degasser, a quaternary pump, and an autosampler was used. Injection volume was 10 µL for all samples. LC and MS conditions were in

accordance to Wissenbach et al. with minor modifications [7]. Gradient elution was performed on a TF Hypersil GOLD C18 column (100×2.1 mm, 1.9 μm) using 10 mM aqueous ammonium formate plus 0.1% formic acid pH 3.4 (eluent A) and acetonitrile plus 0.1% formic acid (eluent B). The flow rate was set to 0.5 mL/min, and the gradient was programmed as follows: 0–1.0 min 2% B, 1.0–3.0 min to 10% B, 3.0–5.0 min to 15% B, 5.0–7.5 min to 20% B, 7.5–10.0 min to 25% B, 10.0–11.5 min to 30% B, 11.5–13.0 min to 35% B, 13.0–14.5 min to 50% B, 14.5–16.0 min to 60% B, 16.0–19.0 min to 90% B, and 19.0–21.0 hold 90% B followed by column flushing and reequilibration. The injection volume for all samples was 10 μL each. The MS conditions were as follows: polarity, positive; sheath gas, nitrogen at flow rate of 34 AU; auxiliary gas, nitrogen at flow rate of 11 AU; vaporizer temperature, 250 °C; source voltage, 3.00 kV; ion transfer capillary temperature, 300 °C; capillary voltage, 38 V; and tube lens voltage, 110 V. AGC was set to 15,000 ions for full scan and 5,000 ions for MS^n. The maximum IT for full scan (MS^1 stage) was set to 100 ms, spectrum data type, profile. Collision-induced dissociation (CID)-MS^n experiments were performed on precursor ions selected from MS^1 using DDA: MS^1 was performed in the full scan mode (*m/z* 100–800). MS^2 and MS^3 were performed in the DDA mode: four DDA MS^2 scan filters were chosen to provide MS^2 on the four most intense signals from MS^1, and additionally, eight MS^3 scan filters were chosen to record MS^3 on the most and second most intense signals from the MS^2. MS^2 spectra were collected with a higher priority than MS^3 spectra. Normalized wideband collision energies were 35.0% for MS^2 and 40.0% for MS^3. Other settings were as follows for MS^2: minimum signal threshold, 100 counts; isolation width, 1.5 u; for MS^3: minimum signal threshold, 50 counts; isolation width, 2.0 u; for both stages: activation Q, 0.25; activation time, 30 ms; and dynamic exclusion mode: repeat count, 2; repeat duration, 15 s; exclusion list size, 50; exclusion duration, 15 s.

Results and discussion

Identification of metabolites in vivo and in vitro

The phase I and II metabolites of 4-CEC, ephylone, NEH, and 4F-PHP identified in authentic human biosamples or pS9 incubations by means of LC-HRMS/MS are summarized in the Electronic Supplementary Material (ESM) in Table S1. The information whether a metabolite was detected in plasma, urine and/or the in vitro incubations can be taken from Table S2 (ESM). The precursor ion (PI) mass recorded in MS^1, characteristic fragment ions (FI) in MS^2, relative intensities in MS^2, calculated exact masses, elemental compositions, deviation of the measured from the calculated masses, and retention times (RT) are also given. Metabolites were sorted by increasing mass and RT and assigned to a unique Metabolite ID. In total, nine metabolites of 4-CEC, 17 of ephylone, 11 of NEH, and 10 of 4F-PHP were tentatively identified. Furthermore, four pairs of diastereomers were identified (M12/13, M18/19, M37/38, M48/49). Absolute peak areas of 4-CEC, ephylone, NEH, 4F-PHP, and their phase I and II metabolites in MS^1 (positive ionization mode, ESI +) derived from analyses of authentic human biosamples and pS9 incubations by LC-HRMS/MS are summarized in Table S2 (ESM). Parent compounds or metabolites identified in authentic human urine by means of GC-MS are given in Table S3 (ESM). Neither parent compound nor metabolites were detectable in the plasma sample by GC-MS.

Because the number of NPS is constantly increasing, rapid and cost-effective methods are needed to study the metabolism of these compounds in order to develop suitable toxicological screening procedures. In vitro studies for example based on pS9 incubations provide a rapid way of generating an overview of the metabolic pathways [3, 15, 9, 16]. The presence of these preliminary metabolites should further be confirmed in vivo. For this purpose, animal models such as rats, pigs, or zebrafish larvae can be used, but species differences have to be considered [17-19]. An intake by humans in the framework of a controlled trial would be the gold standard, but is considered as unethical, time-consuming, and expensive. However, in rare cases, human biosamples after intake of NPS derived from authentic cases are available as presented in this study. These specimens were kept frozen until analysis as lowered temperature was shown to enhance stability of cathinones in blood samples [20]. MS-based procedures proved to be suitable for metabolism studies due to high flexibility, sensitivity, and selectivity. Especially HR devices are promising tools for identification

of unknown compounds [21], but rather expensive and not available in every toxicological laboratory. Therefore, the detectability of the four synthetic cathinones and/or their metabolites in human biosamples by GC-MS was also investigated. For all compounds, LC-HRMS^1 data was screened for potential exact PI masses of expected metabolites in the first step. Afterwards, the fragmentation pattern in the MS^2 spectrum was interpreted and compared to that of the parent compound for tentative identification. Due to the high number of metabolites, the fragmentation patterns could not be discussed in detail for all metabolites and only the typical FI used for identification will be discussed. Only the calculated exact masses will be used in this chapter.

As described by Niessen and Correa [22], loss of water (-18.0106 u, H_2O) is characteristic for the fragmentation pattern of cathinones, but not pyrrolidinophenones. The spectra of 4-CEC, ephylone, NEH, and most of their metabolites contained intense FI after initial water loss, while the 4F-PHP spectrum did not contain such a FI as given in Table S1 (ESM). In case of 4-CEC (PI at *m/z* 212.0837, $C_{11}H_{15}ONCl$), loss of water resulted in the FI at *m/z* 194.0731 ($C_{11}H_{13}NCl$) and the most intense FI at *m/z* 159.1043 was formed after subsequent loss of a chlorine radical (-34.9688). Both FI were shifted by -28.0313 u (C_2H_4) in the *N*-deethyl 4-CEC (M1) spectrum. After reduction of the carbonyl group (M3), water loss resulted in the most intense FI at *m/z* 196.0888. Due to the used HR device, the PI mass of M3 (*m/z* 214.0993) could be distinguished from the $2C^{13}$ isotope (*m/z* 214.0903) and the Cl^{37} isotope (*m/z* 214.0807) of 4-CEC. M3 was also detected as glucuronide (M9). Furthermore, conjugates of M1 and dicarboxylic acids, by name malonic acid, succinic acid, and glutaric acid, could be detected (M6-8). Analysis in negative ionization mode confirmed these findings (see ESM, Table S1). In rat urine, conjugates of mephedrone and methylone metabolites with succinic, glutaric, and adipic acid were previously detected [23, 24]. Nor-mephedrone succinate was also described to be present in human plasma and urine [25, 26]. However, to our knowledge, this is the first report of a synthetic cathinone metabolite bound to malonic acid and the first detection of a synthetic cathinone metabolite conjugate with glutaric acid in human urine. No dicarboxylic acid conjugates of ephylone, NEH, and 4F-PHP metabolites could be detected.

Seventeen ephylone metabolites were detected, including the four phase I metabolites previously described by Krotulski et al. [5] . However, abundances of the metabolites (see ESM, Table S2) underline the importance of the additional identification of phase II metabolites. Eleven NEH metabolites could be identified including the only *N*-acetyl metabolite in this study, *N*-deethyl *N*-acetyl NEH (M32) and 10 4F-PHP metabolites were detected. All in all, metabolic pathways were comparable to the ones described for other synthetic cathinones [4].

Four pairs of diastereomers were identified. The reduction of the carbonyl group formed two diastereomeric alcohols. Mass spectra within each pair of diastereomers were very similar as already described by Uralets et al. for other diastereomers of reduced cathinones [27]. Not always after carbonyl reduction, two diastereomers could be detected. Possible explanations could be an insufficient separation by the used LC system or stereospecific formation in varying quantities.

4-CEC, ephylone, NEH, and five metabolites were detectable in the urine sample by GC-MS (see ESM, Table S3). The low number of detected metabolites and the negative screening result in plasma was potentially caused by insufficient volatility or quantity of the analytes and sensitivity of the used GC-MS apparatus.

In order to identify suitable screening targets, absolute peak areas of 4-CEC, ephylone, NEH, 4F-PHP, and their phase I and II metabolites derived from LC-HRMS/MS analyses of authentic human biosamples and pS9 incubations are given in Table S2 (ESM). Targets detected by GC-MS are given in Table S3 (ESM). For all four synthetic cathinones, the parent compound was amongst the most abundant signals in plasma and/or urine and should therefore be included in the screening procedure. For 4-CEC, the dihydro metabolite (M3), also in combination with *N*-deethylation (M2), could be recommended as additional target for LC-, and the corresponding acetylated metabolites for GC-based screening approaches. If no conjugate cleavage is performed during sample preparation, demethylenyl ephylone glucuronide (M26), with or without methylation (M27/28), should be considered for LC-based screening, otherwise the corresponding aglyca (M15-17), also for GC-MS as acetylated compounds. Only the parent compound NEH was detectable in urine by GC-MS, while 4F-PHP was not detectable in biosamples by GC-MS at all. However, suitable

targets for LC-based screenings should be *N*-deethyl and hydroxy NEH (M29 and M33), as well as oxo 4F-PHP (M43 and M44). With exception of M43, all of these recommended targets were also detectable in the pS9 incubations and structures are given in Figure 2. As given in Table S2, a lower number of metabolites were detected in pS9 incubations in comparison to human biosamples. This was most probably caused by the lack of distribution and elimination processes in in vitro models, which could also lead to minor formation of metabolites in concentrations under the detection limit. Furthermore, pS9 was incubated for a maximum of 360 min, while time between intake and sampling of blood and urine may have been longer. Nevertheless, these findings are based on only one authentic case and should be considered as possible limitation.

Involvement of monooxygenases in phase I metabolic reactions

In order to identify the monooxygenases involved in the synthetic cathinones' phase I metabolic transformations, a monooxygenases activity screening was conducted consisting of incubations with one out of the ten most abundant CYP isoforms in human liver or FMO3. Incubations with pHLM were used as positive control to confirm suitable incubation conditions by metabolite formation. Results are summarized in Table 1. In case of all four synthetic cathinones, the dihydro metabolites (M3, M18, M31, M42) were only detected in pHLM incubations, but not in incubations with the recombinant monooxygenases. Therefore, the monooxygenase isoforms tested in this monooxygenases activity screening are not expected to catalyze the formation of the dihydro metabolites of 4-CEC, ephylone, NEH, and 4F-PHP. CYP2C19 was found to be involved in the formation of the *N*-deethyl metabolites of 4-CEC, ephylone, and NEH (M1, M10, M29), as well as in the *N,N*-dealkyl metabolite formation of 4F-PHP (M41). Depending on the synthetic cathinone, CYP1A2, CYP2B6, or CYP3A4 were also involved in the *N*-deethylation or *N,N*-dealkylation. Hydroxylamines were only detectable in incubations with 4-CEC (M4) and ephylone (M21) and their formation was catalyzed by CYP1A2 (only 4-CEC), CYP3A4, and FMO3. The formation of demethylenyl ephylone (M15) was catalyzed by CYP1A2, CYP2C19, and CYP2D6 and of hydroxy ephylone (M20) only by CYP3A4. Both hydroxy NEH isomers (M33, M34) were only formed in

CYP1A2 incubations. CYP1A2 also catalyzed the formation of two hydroxy 4F-PHP isomers, while CYP2C19 and CYP3A4 formed all three isomers (M45-46). Oxo 4F-PHP (M44) was formed in incubations with CYP1A2, CYP2B6, and CYP3A4.

In case of 4-CEC, ephylone, and 4F-PHP, at least four different monooxygenase isoforms were involved in the phase I metabolic transformations. Therefore, an inhibition of a single isoform in case of a drug-drug interaction or interindividual expression differences are not expected to have a significant influence on their concentrations, in contrast to NEH, where only two CYP isoforms were found to be involved in the phase I metabolic reactions. Especially an inhibition of CYP1A2 would lead to almost complete inhibition of initial metabolic steps and could therefore cause a significant increase in NEH levels and toxicity.

Determination of plasma concentrations

Standard addition method was used and the authentic plasma sample analyzed without or with addition of the four synthetic cathinones resulting in final plasma concentrations of additionally 2, 4, 6, 8, and 10 ng/mL respectively. In Figure 3, the analyte concentration is plotted versus the peak area ratio of analyte and internal standard. The data points on the y-axis represent the analyte amount in the native plasma sample and after linear regression, the following plasma concentrations were determined: 1.9 ng/mL 4-CEC, 8.5 ng/mL ephylone, 1.0 ng/mL NEH, and 0.8 ng/mL 4F-PHP. Unfortunately, dosage and time of intake were unknown. No plasma concentrations were published for 4-CEC, NEH, and 4F-PHP, so far. Published ephylone concentrations in toxicological death investigations and drugged driving casework ranged from 12 to 1,200 ng/mL [5]. Therefore, plasma concentrations determined in the presented case can be considered as low. This assumption was confirmed by the patient's health status including hospital discharge after one only day and comparison to published concentrations of other synthetic cathinones [4].

Metabolic stability in pHLM incubations

Metabolic stability in pHLM incubations is depicted in Figure 4 and in vitro half-life ($t_{1/2}$) values, calculated microsomal intrinsic clearances ($CL_{int,micr}$), and intrinsic clearances (CL_{int}) are summarized in Table 2. The shortest $t_{1/2}$ was determined for 4F-PHP with 38 min. The other compounds provided $t_{1/2}$ between 85 and 105 min. The highest CL_{int} of 15.7 mL× min^{-1}×kg^{-1} was determined for 4F-PHP, other CL_{int} were between 5.7 and 7.0 mL× min^{-1}×kg^{-1}.

Metabolic stability was determined based on disappearance of the test compound during incubation with pHLM and expressed as $t_{1/2}$, $CL_{int,micr}$, and CL_{int}. The latter was calculated by scaling $CL_{int,micr}$ to whole liver dimensions. CL_{int} is defined as the maximum activity of the liver towards a drug in the absence of other physiological determinants such as hepatic blood flow and drug binding within the blood matrix [12]. In general, the protein concentrations should be minimized to ensure the absence of non-specific protein binding and the concentration of a test compound during the incubation should be below the Michaelis-Menten constant (K_m). As there was no information on K_m values for the tested cathinones available, a preferably low concentration was used in the assay as recommended by Baranczewski et al. [12]. Non-metabolic degradation of the synthetic cathinones could be excluded by control incubations without pHLM and subsequent t-tests that did not show a significant difference in the natural logarithms of the peak area ratios of incubations after 0 min and control incubations.

According to McNaney et al. [28], 4F-PHP could be classified as intermediate clearance compound and 4-CEC, ephylone, and NEH as low clearance compounds. The determined values were comparable to the ones published for PV8 and 4-methoxy-α-PVP [29, 30]. However, CL_{int} of synthetic cathinones were much lower than the ones determined for synthetic cannabinoid receptor agonists [31, 32].

Conclusions

In total, 47 metabolites of 4-CEC, ephylone, NEH, and 4F-PHP were identified in human biosamples and pS9 incubations including conjugates with dicarboxylic acids that were not described to be present in human urine before. Suitable targets for the development of screening

procedures were recommended. As various monooxygenases were shown to be involved in the initial metabolic steps, interactions with other drugs (of abuse) based on enzyme inhibition should be unlikely, except for NEH where only CYP1A2 and CYP2C19 were involved. Due to the health status of the patient, the determined plasma concentrations between 0.8 and 8.5 ng/mL are expected to be rather low and not life-threatening. In vitro half-life values and intrinsic clearances indicated that these synthetic cathinones can be classified as intermediate (4F-PHP) or low (4-CEC, ephylone, and NEH) clearance compounds, comparable to other synthetic cathinones' clearances. In summary, the present work clearly expanded the knowledge about the toxicokinetics of the four synthetic cathinones and may help clinical and forensic toxicologists to reliably detect these compounds in human biosamples and interpret their findings.

Electronic supplementary material

Supplementary material may be found online.

Acknowledgements

The authors like to thank Daniel Arnold, Nora Toggweiler and Armin A. Weber for their support and/or helpful discussion and Thermo Fisher Scientific for providing a seed unit of the apparatus.

Compliance with ethical standards

Conflict of interest

The authors declare that they have no conflict of interest.

Ethical approval

This article does not contain any studies with human participants or animals performed by any of the authors. The human material investigated was submitted to the authors´ laboratory for regular toxicological analysis.

References

1. UNODC. World Drug Report 2018. Booklet 3. Analysis of drug markets - opioids, cocaine, cannabis, synthetic drugs. In: UNODC, editor.: United Nations publication; 2018.
2. EMCDDA. European Drug Report 2018. Publications of of the European Union 2018.
3. Tyrkko E, Andersson M, Kronstrand R (2016) The Toxicology of New Psychoactive Substances: Synthetic Cathinones and Phenylethylamines. Ther Drug Monit; 38:190 - 216
4. Ellefsen KN, Concheiro M, Huestis MA (2016) Synthetic cathinone pharmacokinetics, analytical methods, and toxicological findings from human performance and postmortem cases. Drug Metab Rev; 48:237 - 65
5. Krotulski AJ, Papsun DM, De Martinis BS, Mohr ALA, Logan BK (2018) N-Ethyl Pentylone (Ephylone) Intoxications: Quantitative Confirmation and Metabolite Identification in Authentic Human Biological Specimens. J Anal Toxicol; 42:467 - 75
6. Helfer AG, Michely JA, Weber AA, Meyer MR, Maurer HH (2017) Liquid chromatography-high resolution-tandem mass spectrometry using Orbitrap technology for comprehensive screening to detect drugs and their metabolites in blood plasma. Anal Chim Acta; 965:83 - 95
7. Wissenbach DK, Meyer MR, Remane D, Philipp AA, Weber AA, Maurer HH (2011) Drugs of abuse screening in urine as part of a metabolite-based LC-MSn screening concept. Anal Bioanal Chem; 400:3481 - 9
8. Maurer HH, Pfleger K, Weber AA. Mass spectral data of drugs, poisons, pesticides, pollutants and their metabolites. Weinheim: Wiley-VCH; 2016.
9. Richter LHJ, Maurer HH, Meyer MR (2017) New psychoactive substances: Studies on the metabolism of XLR-11, AB-PINACA, FUB-PB-22, 4-methoxy-alpha-PVP, 25-I-NBOMe, and meclonazepam using human liver preparations in comparison to primary human hepatocytes, and human urine. Toxicol Lett; 280:142 - 50
10. Chauret N, Gauthier A, Nicoll-Griffith DA (1998) Effect of common organic solvents on in vitro cytochrome P450-mediated metabolic activities in human liver microsomes. Drug Metab Dispos; 26:1 - 4
11. Wagmann L, Meyer MR, Maurer HH (2016) What is the contribution of human FMO3 in the N-oxygenation of selected therapeutic drugs and drugs of abuse? Toxicol Lett; 258:55 - 70
12. Baranczewski P, Stanczak A, Sundberg K, Svensson R, Wallin A, Jansson J et al. (2006) Introduction to in vitro estimation of metabolic stability and drug interactions of new chemical entities in drug discovery and development. Pharmacol Rep; 58:453 - 72
13. Davies B, Morris T (1993) Physiological parameters in laboratory animals and humans. Pharm Res; 10:1093 - 5
14. Michely JA, Meyer MR, Maurer HH (2018) Power of Orbitrap-based LC-high resolution-MS/MS for comprehensive drug testing in urine with or without conjugate cleavage or using dried urine spots after on-spot cleavage in comparison to established LC-MS(n) or GC-MS procedures. Drug Test Anal; 10:158 - 63
15. Richter LHJ, Flockerzi V, Maurer HH, Meyer MR (2017) Pooled human liver preparations, HepaRG, or HepG2 cell lines for metabolism studies of new psychoactive substances? A study using MDMA, MDBD, butylone, MDPPP, MDPV, MDPB, 5-MAPB, and 5-API as examples. J Pharm Biomed Anal; 143:32 - 42
16. Wagmann L, Richter LHJ, Kehl T, Wack F, Bergstrand MP, Brandt SD et al. (2019) In vitro metabolic fate of nine LSD-based new psychoactive substances and their analytical detectability in different urinary screening procedures. Anal Bioanal Chem; doi: 10.1007/s00216-018-1558-9
17. Schaefer N, Wojtyniak JG, Kettner M, Schlote J, Laschke MW, Ewald AH et al. (2016) Pharmacokinetics of (synthetic) cannabinoids in pigs and their relevance for clinical and forensic toxicology. Toxicol Lett; 253:7 - 16

18. Caspar AT, Westphal F, Meyer MR, Maurer HH (2018) LC-high resolution-MS/MS for identification of 69 metabolites of the new psychoactive substance 1-(4-ethylphenyl-)-N-[(2-methoxyphenyl)methyl] propane-2-amine (4-EA-NBOMe) in rat urine and human liver S9 incubates and comparison of its screening power with further MS techniques. Anal Bioanal Chem; 410:897 - 912

19. Richter LHJ, Herrmann J, Andreas A, Park YM, Wagmann L, Flockerzi V et al. (2019) Tools for studying the metabolism of new psychoactive substances for toxicological screening purposes - A comparative study using pooled human liver S9, HepaRG cells, and zebrafish larvae. Toxicol Lett; 305:73 - 80

20. Sorensen LK (2011) Determination of cathinones and related ephedrines in forensic whole-blood samples by liquid-chromatography-electrospray tandem mass spectrometry. J Chromatogr B Analyt Technol Biomed Life Sci; 879:727 - 36

21. Wagmann L, Maurer HH (2018) Bioanalytical Methods for New Psychoactive Substances. Handb Exp Pharmacol; 252:413 - 39

22. Niessen WM, Correa RA. Interpretation of MS-MS Mass Spectra of Drugs and Pesticides. Hoboken, New Jersey: John Wiley & Sons; 2016.

23. Linhart I, Himl M, Zidkova M, Balikova M, Lhotkova E, Palenicek T (2016) Metabolic profile of mephedrone: Identification of nor-mephedrone conjugates with dicarboxylic acids as a new type of xenobiotic phase II metabolites. Toxicol Lett; 240:114 - 21

24. Zidkova M, Linhart I, Balikova M, Himl M, Dvorackova V, Lhotkova E et al. (2018) Identification of three new phase II metabolites of a designer drug methylone formed in rats by N-demethylation followed by conjugation with dicarboxylic acids. Xenobiotica; 48:618 - 25

25. Pozo OJ, Ibanez M, Sancho JV, Lahoz-Beneytez J, Farre M, Papaseit E et al. (2015) Mass spectrometric evaluation of mephedrone in vivo human metabolism: identification of phase I and phase II metabolites, including a novel succinyl conjugate. Drug Metab Dispos; 43:248 - 57

26. Olesti E, Farre M, Papaseit E, Krotonoulas A, Pujadas M, de la Torre R et al. (2017) Pharmacokinetics of Mephedrone and Its Metabolites in Human by LC-MS/MS. AAPS J; 19:1767 - 78

27. Uralets V, Rana S, Morgan S, Ross W (2014) Testing for designer stimulants: metabolic profiles of 16 synthetic cathinones excreted free in human urine. J Anal Toxicol; 38:233-41

28. McNaney CA, Drexler DM, Hnatyshyn SY, Zvyaga TA, Knipe JO, Belcastro JV et al. (2008) An automated liquid chromatography-mass spectrometry process to determine metabolic stability half-life and intrinsic clearance of drug candidates by substrate depletion. Assay Drug Dev Technol; 6:121-9

29. Ellefsen KN, Wohlfarth A, Swortwood MJ, Diao X, Concheiro M, Huestis MA (2016) 4-Methoxy-alpha-PVP: in silico prediction, metabolic stability, and metabolite identification by human hepatocyte incubation and high-resolution mass spectrometry. Forensic Toxicol; 34:61 - 75

30. Swortwood MJ, Ellefsen KN, Wohlfarth A, Diao X, Concheiro-Guisan M, Kronstrand R et al. (2016) First metabolic profile of PV8, a novel synthetic cathinone, in human hepatocytes and urine by high-resolution mass spectrometry. Anal Bioanal Chem; 408:4845 - 56

31. Mardal M, Gracia-Lor E, Leibnitz S, Castiglioni S, Meyer MR (2016) Toxicokinetics of new psychoactive substances: plasma protein binding, metabolic stability, and human phase I metabolism of the synthetic cannabinoid WIN 55,212-2 studied using in vitro tools and LC-HR-MS/MS. Drug Test Anal; 8:1039 - 48

32. Gandhi AS, Wohlfarth A, Zhu M, Pang S, Castaneto M, Scheidweiler KB et al. (2015) High-resolution mass spectrometric metabolite profiling of a novel synthetic designer drug, N-(adamantan-1-yl)-1-(5-fluoropentyl)-1H-indole-3-carboxamide (STS-135), using cryopreserved human hepatocytes and assessment of metabolic stability with human liver microsomes. Drug Test Anal; 7:187 - 98

Legends to the figures

Figure 1. Chemical structures of the investigated synthetic cathinones.

Figure 2. Chemical structures of metabolites recommended as screening targets for liquid chromatography-based urine screenings.

Figure 3. Obtained standard addition calibration curves after addition of 0, 2, 4, 6, 8, or 10 ng/mL 4-CEC, ephylone, NEH, and 4F-PHP to authentic human plasma after unknown dose and time of consumption. Analyte concentration is plotted versus peak area ratios of analyte and internal standard (trimipramine-d_3).

Figure 4. Metabolic stability of 4-CEC (A), ephylone (B), NEH (C), and 5F-PHP (D) in incubations with pooled human liver microsomes (pHLM). Incubation time is plotted versus the natural logarithm of the peak area ratios of the analyte and the internal standard (IS). Points indicate mean values (n = 2). $t_{1/2}$, in vitro half-life

Table 1. General involvement of monooxygenases in the formation of the given 4-CEC, ephylone, NEH, and 4F-PHP metabolites. Pooled human liver microsomes (pHLM) incubations were used as positive control. Metabolite IDs correspond to Table S1. CYP, cytochrome P450; FMO, flavin-containing monooxygenase, +, detected; -, not detected

Parent compound	CYP										FMO3	pHLM
Metabolite ID	1A2	2A6	2B6	2C8	2C9	2C19	2D6	2E1	3A4	3A5		
4-CEC												
M1 (*N*-deethyl-)	+	-	+	-	-	+	-	-	-	-	-	+
M3 (dihydro-)	-	-	-	-	-	-	-	-	-	-	-	+
M4 (hydroxylamine)	+	-	-	-	-	-	-	-	+	-	+	+
Ephylone												
M10 (*N*-deethyl-)	-	-	+	-	-	+	-	-	+	-	-	+
M15 (demethylenyl-)	+	-	-	-	-	+	+	-	-	-	-	+
M18 (dihydro-)	-	-	-	-	-	-	-	-	-	-	-	+
M20 (hydroxy-)	-	-	-	-	-	-	-	-	+	-	-	+
M21 (hydroxylamine)	-	-	-	-	-	-	-	-	+	-	+	+
NEH												
M29 (*N*-deethyl-)	+	-	-	-	-	+	-	-	-	-	-	+
M31 (dihydro-)	-	-	-	-	-	-	-	-	-	-	-	+
M33 (hydroxy-)	+	-	-	-	-	-	-	-	-	-	-	+
M34 (hydroxy-)	+	-	-	-	-	-	-	-	-	-	-	+
4F-PHP												
M41 (*N,N*-dealkyl-)	+	-	+	-	-	+	-	-	+	-	-	+
M42 (dihydro-)	-	-	-	-	-	-	-	-	-	-	-	+
M44 (oxo-)	+	-	+	-	-	-	-	-	+	-	-	+
M45 (hydroxy-)	+	-	-	-	-	+	-	-	-	-	-	+
M46 (hydroxy-)	+	-	-	-	-	+	-	-	-	-	-	+
M47 (hydroxy-)	-	-	+	-	-	+	-	-	-	-	-	+

Table 2. Metabolic stability of 4-CEC, ephylone, NEH, and 4F-PHP in pooled human liver microsomes (pHLM) incubations expressed as in vitro half-life ($t_{1/2}$) and calculated microsomal intrinsic clearance ($CL_{int,\ micr}$) and intrinsic clearance (CL_{int}).

Compound	$t_{1/2}$, min	$CL_{int,\ micr}$, mL× min^{-1}×mg^{-1}	CL_{int}, mL× min^{-1}×kg^{-1}
4-CEC	105	0.0066	5.7
Ephylone	96	0.0072	6.2
NEH	85	0.0082	7.0
4F-PHP	38	0.0182	15.7

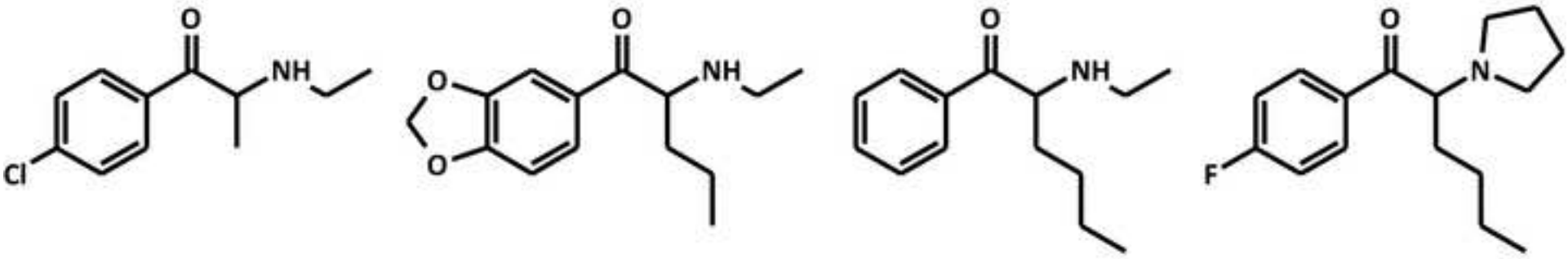

4-CEC Ephylone NEH 4F-PHP

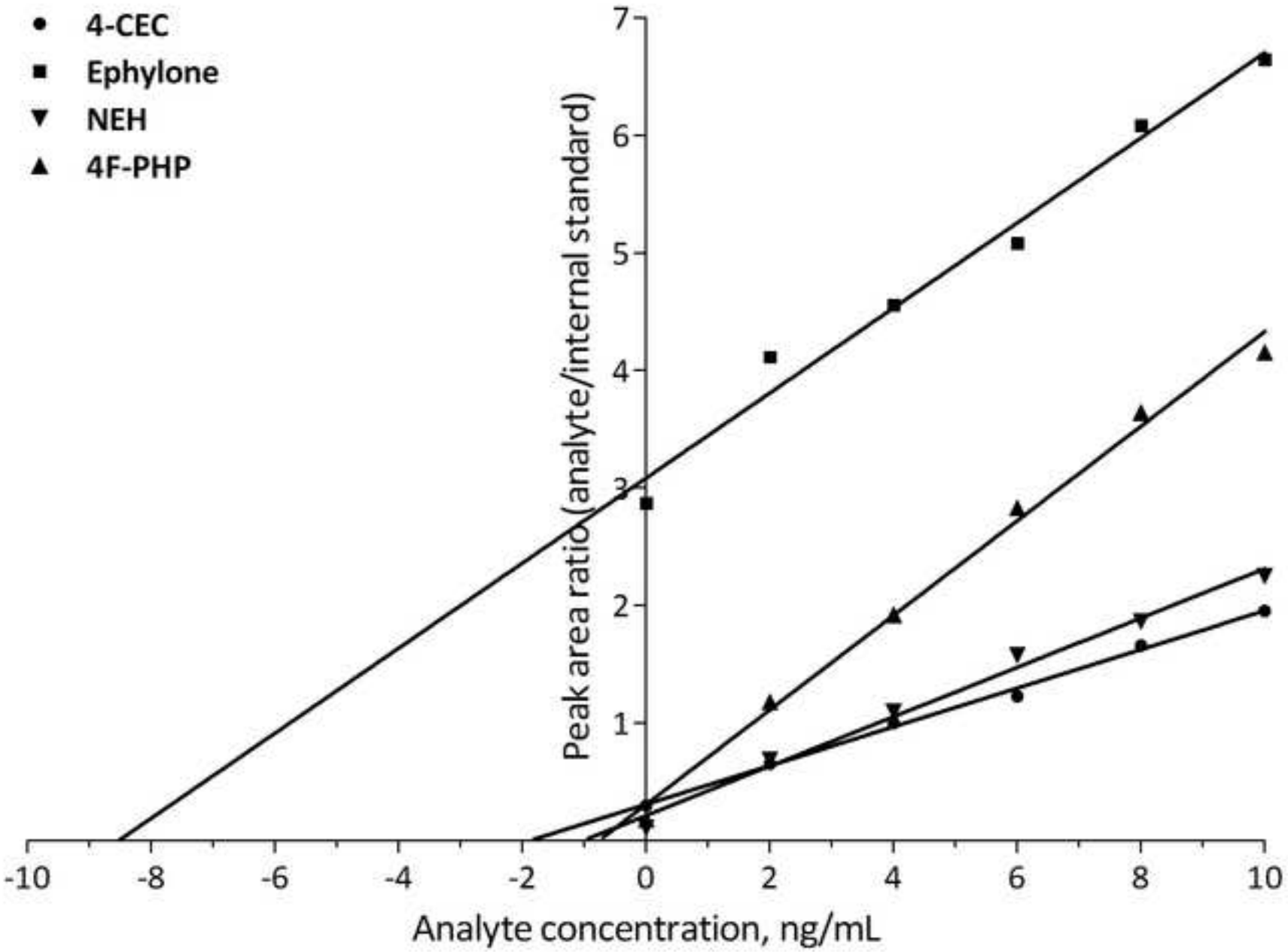
4-CEC
Ephylone
NEH
4F-PHP
Peak area ratio (analyte/internal standard)
7
6
5
4
3
2
1
-10
-8
-6
-4
-2
0
2
4
6
8
10
Analyte concentration, ng/mL

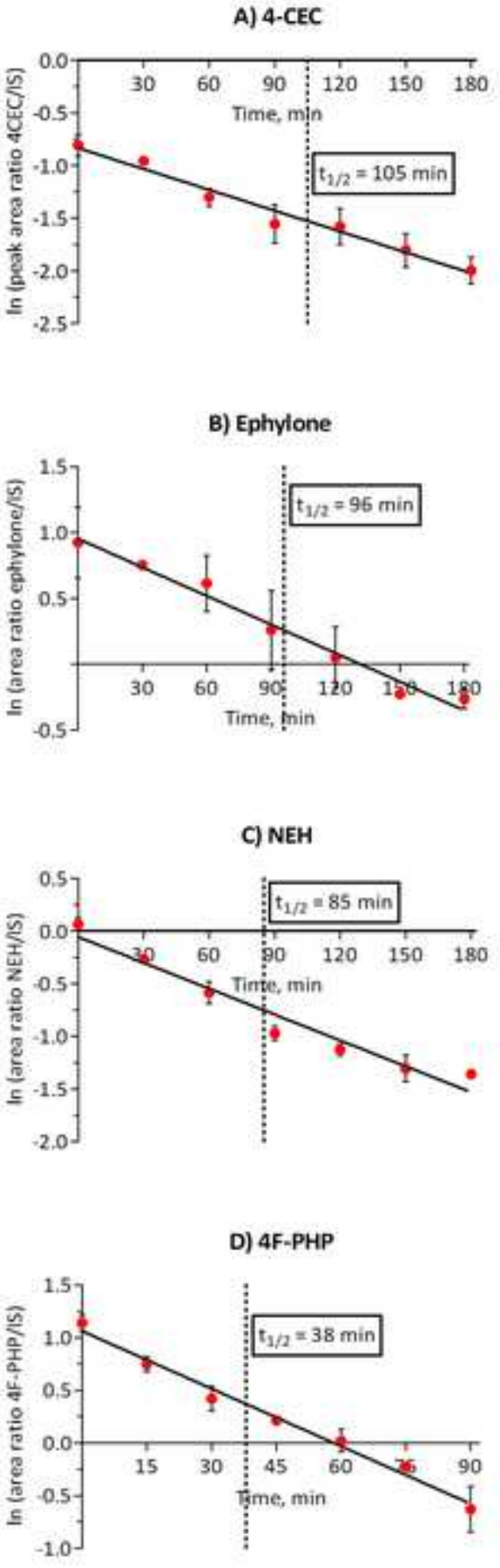

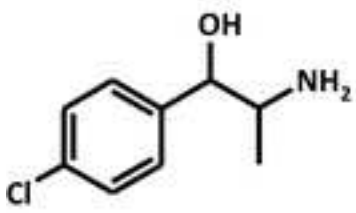

M2

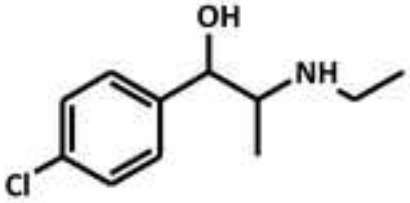

M3

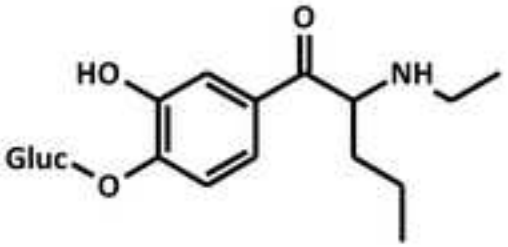

M25/26

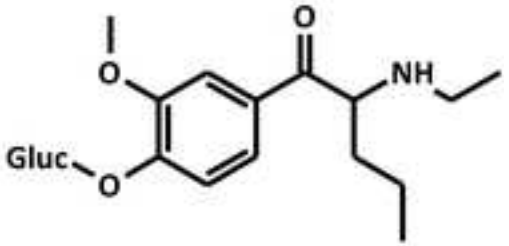

M27/28

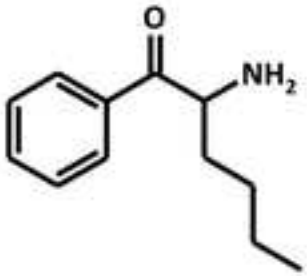

M29

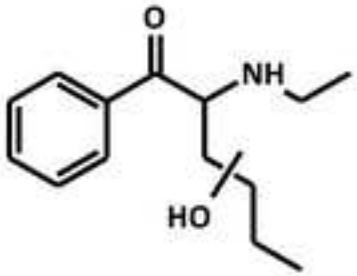

M33

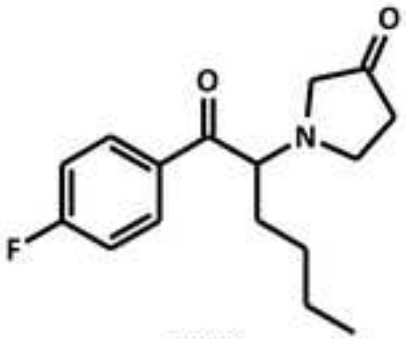

M43

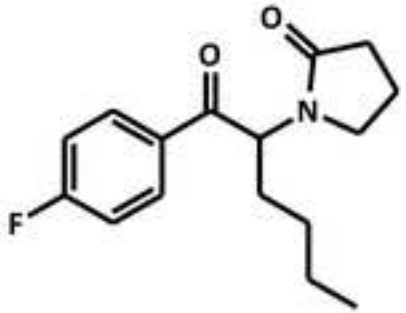

M44

Forensic Toxicology

Electronic Supplementary Material

Toxicokinetic studies of the four new psychoactive substances 4-chloroethcathinone, *N*-ethylnorpentylone, *N*-ethylhexedrone, and 4-fluoro-alpha-pyrrolidinohexiophenone

Table S1. 4-CEC, ephylone, NEH, 4F-PHP, and their phase I and II metabolites identified in authentic human biosamples or pS9 incubations by means of LC-HRMS/MS together with the used ionization mode, precursor ion (PI) mass recorded in MS^1, characteristic fragment ions (FI) in MS^2, relative intensities in MS^2, calculated exact masses, elemental compositions, deviation of the measured from the calculated masses, and retention times (RT). Metabolites were sorted by increasing mass and RT. ESI+, positive electrospray ionization mode; ESI-, negative electrospray ionization mode

Metabolite ID	Metabolic reaction	Ionization mode	Measured masses of PI and characteristic FI, *m/z*	Relative intensity in MS^2, %	Calculated Exact Masses, *m/z*	Elemental composition	Error, ppm	RT, min
4-CEC (parent compound)	-	ESI +	PI at *m/z* 212.0837	26	212.0837	$C_{11}H_{15}ONCl$	0.00	3.93
			FI at *m/z* 194.0732	86	194.0731	$C_{11}H_{13}NCl$	0.52	
			FI at *m/z* 166.0417	25	166.0424	C_9H_9NCl	-4.22	
			FI at *m/z* 159.1043	100	159.1043	$C_{11}H_{13}N$	0.00	
			FI at *m/z* 144.0808	32	144.0813	$C_{10}H_{10}N$	-3.47	
			FI at *m/z* 139.0309	15	139.0309	C_8H_8Cl	0.00	
			FI at *m/z* 131.0731	17	131.0730	C_9H_9N	0.76	
M1	*N*-Deethylation	ESI +	PI at *m/z* 184.0519	2	184.0524	$C_9H_{11}ONCl$	-2.72	3.35
			FI at *m/z* 167.0258	9	167.0258	C_9H_8OCl	0.00	
			FI at *m/z* 166.0417	42	166.0418	C_9H_9NCl	-0.60	
			FI at *m/z* 139.0307	19	139.0309	C_8H_8Cl	-1.44	
			FI at *m/z* 131.0729	100	131.0730	C_9H_9N	-0.76	
			FI at *m/z* 103.0546	7	103.0542	C_8H_7	3.88	
M2	*N*-Deethylation + reduction	ESI +	PI at *m/z* 186.0675	1	186.0680	$C_9H_{13}ONCl$	-2.69	3.33
			FI at *m/z* 168.0566	100	168.0575	$C_9H_{11}NCl$	-5.36	
			FI at *m/z* 151.0301	29	151.0309	C_9H_8Cl	-5.30	
			FI at *m/z* 133.0880	15	133.0886	$C_9H_{11}N$	-4.51	
			FI at *m/z* 116.0617	32	116.0621	C_9H_8	-3.45	
M3	Reduction	ESI +	PI at *m/z* 214.0990	2	214.0993	$C_{11}H_{17}ONCl$	-1.40	4.03
			FI at *m/z* 196.0885	100	196.0888	$C_{11}H_{15}NCl$	-1.53	
			FI at *m/z* 168.0571	8	168.0575	$C_9H_{11}NCl$	-2.38	
			FI at *m/z* 151.0307	7	151.0309	C_9H_8Cl	-1.32	
			FI at *m/z* 133.0886	2	133.0886	$C_9H_{11}N$	0.00	
			FI at *m/z* 116.0622	10	116.0621	C_9H_8	0.86	
M4	*N*-Oxygenation	ESI +	PI at *m/z* 228.0783	7	228.0786	$C_{11}H_{15}O_2NCl$	-1.32	5.20
			FI at *m/z* 210.0678	2	210.0680	$C_{11}H_{13}ONCl$	-0.95	
			FI at *m/z* 175.0991	5	175.0992	$C_{11}H_{13}ON$	-0.57	
			FI at *m/z* 138.9945	100	138.9945	C_7H_4OCl	0.00	
			FI at *m/z* 131.0730	8	131.0730	C_9H_9N	0.00	
M5	Carboxylation	ESI +	PI at *m/z* 242.0590	11	242.0578	$C_{11}H_{13}O_3NCl$	4.96	3.88
			FI at *m/z* 224.0462	25	224.0473	$C_{11}H_{11}O_2NCl$	-4.91	
			FI at *m/z* 196.0517	11	196.0524	$C_{10}H_{11}ONCl$	-3.57	
			FI at *m/z* 178.0410	100	178.0418	$C_{10}H_9NCl$	-4.49	
			FI at *m/z* 168.0569	16	168.0575	$C_9H_{11}NCl$	-3.57	
			FI at *m/z* 125.0148	36	125.0153	C_7H_6Cl	-4.00	
M6	*N*-Deethylation + malonylation	ESI +	PI at *m/z* 270.0523	5	270.0528	$C_{12}H_{13}O_4NCl$	-1.85	5.38
			FI at *m/z* 252.0419	28	252.0422	$C_{12}H_{11}O_3NCl$	-1.19	
			FI at *m/z* 210.0315	5	210.0316	$C_{10}H_9O_2NCl$	-0.48	
			FI at *m/z* 184.0522	46	184.0524	$C_9H_{11}ONCl$	-1.09	

			FI at *m/z* 167.0256	24	167.0258	C_9H_8OCl	-1.20	
			FI at *m/z* 166.0416	90	166.0418	C_9H_9NCl	-1.20	
			FI at *m/z* 139.0307	29	139.0309	C_8H_8Cl	-1.44	
			FI at *m/z* 131.0728	100	131.0730	C_9H_9N	-1.53	
			FI at *m/z* 103.0545	7	103.0542	C_8H_7	2.91	
		ESI -	PI at *m/z* 268.0369	6	268.0382	$C_{12}H_{11}O_4NCl$	-4.85	5.38
			FI at *m/z* 224.0473	94	224.0484	$C_{11}H_{11}O_2NCl$	-4.91	
			FI at *m/z* 206.0369	82	206.0378	$C_{11}H_9ONCl$	-4.37	
			FI at *m/z* 112.0390	100	112.0404	$C_5H_6O_2N$	-12.5	
M7	*N*-Deethylation + succinylation	ESI +	PI at *m/z* 284.0675	5	284.0684	$C_{13}H_{15}O_4NCl$	-3.17	5.50
			FI at *m/z* 266.0573	60	266.0578	$C_{13}H_{13}O_3NCl$	-1.88	
			FI at *m/z* 248.0470	10	248.0473	$C_{13}H_{11}O_2NCl$	-1.21	
			FI at *m/z* 220.0518	2	220.0524	$C_{12}H_{11}ONCl$	-2.73	
			FI at *m/z* 184.0522	49	184.0524	$C_9H_{11}ONCl$	-1.09	
			FI at *m/z* 167.0258	38	167.0258	C_9H_8OCl	0.00	
			FI at *m/z* 166.0417	64	166.0418	C_9H_9NCl	-0.60	
			FI at *m/z* 139.0307	100	139.0309	C_8H_8Cl	-1.44	
			FI at *m/z* 131.0729	63	131.0730	C_9H_9N	-0.76	
			FI at *m/z* 103.0545	24	103.0542	C_8H_7	2.91	
		ESI-	PI at *m/z* 282.0537	14	282.0539	$C_{13}H_{13}O_4NCl$	-0.71	5.50
			FI at *m/z* 264.0431	89	264.0433	$C_{13}H_{11}O_3NCl$	-0.76	
			FI at *m/z* 220.0527	100	220.0535	$C_{12}H_{11}ONCl$	-3.64	
			FI at *m/z* 98.0238	33	98.0248	$C_4H_4O_2N$	-10.2	
M8	*N*-Deethylation + glutarylation	ESI +	PI at *m/z* 298.0830	5	298.0841	$C_{14}H_{17}O_4NCl$	-3.69	5.65
			FI at *m/z* 280.0729	100	280.0735	$C_{14}H_{15}O_3NCl$	-2.14	
			FI at *m/z* 262.0622	90	262.0629	$C_{14}H_{13}O_2NCl$	-2.67	
			FI at *m/z* 234.0677	16	234.0680	$C_{13}H_{13}ONCl$	-1.28	
			FI at *m/z* 184.0522	52	184.0524	$C_9H_{11}ONCl$	-1.09	
			FI at *m/z* 167.0255	23	167.0258	C_9H_8OCl	-1.80	
			FI at *m/z* 166.0416	63	166.0418	C_9H_9NCl	-1.20	
			FI at *m/z* 139.0307	99	139.0309	C_8H_8Cl	-1.44	
			FI at *m/z* 131.0728	53	131.0730	C_9H_9N	-1.53	
			FI at *m/z* 103.0545	21	103.0542	C_8H_7	2.91	
		ESI -	PI at *m/z* 296.0684	13	296.0695	$C_{14}H_{15}O_4NCl$	-3.72	5.65
			FI at *m/z* 278.0588	79	278.0589	$C_{14}H_{13}O_3NCl$	-0.36	
			FI at *m/z* 234.0683	100	234.0691	$C_{13}H_{13}ONCl$	-3.42	
			FI at *m/z* 122.0597	33	122.0611	C_7H_8ON	-11.5	
M9	Reduction + glucuronidation	ESI +	PI at *m/z* 390.1296	8	390.1314	$C_{17}H_{25}O_7NCl$	-4.61	3.69
			FI at *m/z* 214.0982	5	214.0993	$C_{11}H_{17}ONCl$	-5.14	
			FI at *m/z* 196.0879	100	196.0888	$C_{11}H_{15}NCl$	-4.59	
			FI at *m/z* 168.0567	6	168.0575	$C_9H_{11}NCl$	-4.76	
			FI at *m/z* 151.0303	5	151.0309	C_9H_8Cl	-3.97	
			FI at *m/z* 116.0619	6	116.0621	C_9H_8	-1.72	
Ephylone (parent compound)	-	ESI +	PI at *m/z* 250.1435	55	250.1438	$C_{14}H_{20}O_3N$	-1.20	4.47
			FI at *m/z* 232.1328	77	232.1332	$C_{14}H_{18}O_2N$	-1.72	
			FI at *m/z* 202.1225	100	202.1226	$C_{13}H_{16}ON$	-0.49	
			FI at *m/z* 175.0752	24	175.0754	$C_{11}H_{11}O_2$	-1.14	
			FI at *m/z* 135.0440	27	135.0441	$C_8H_7O_2$	-0.74	
			FI at *m/z* 100.1125	47	100.1121	$C_6H_{14}N$	4.00	
M10	*N*-Deethylation	ESI +	PI at *m/z* 222.1122	2	222.1125	$C_{12}H_{16}O_3N$	-1.35	4.14
			FI at *m/z* 204.1018	29	204.1019	$C_{12}H_{14}O_2N$	-0.49	
			FI at *m/z* 174.0913	100	174.0913	$C_{11}H_{12}ON$	0.00	
			FI at *m/z* 146.0962	48	146.0964	$C_{10}H_{12}N$	-1.37	
			FI at *m/z* 135.0440	14	135.0441	$C_8H_7O_2$	-0.74	
			FI at *m/z* 72.0815	16	72.0808	$C_4H_{10}N$	9.71	
M11	*N*-Deethylation + demethylenation + methylation isomer 1	ESI +	PI at *m/z* 224.1271	6	224.1281	$C_{12}H_{18}O_3N$	-4.46	2.83
			FI at *m/z* 206.1165	100	206.1176	$C_{12}H_{16}O_2N$	-5.34	
			FI at *m/z* 164.0697	10	164.0706	$C_9H_{10}O_2N$	-5.49	
			FI at *m/z* 150.0543	12	150.0550	$C_8H_8O_2N$	-4.66	
			FI at *m/z* 135.0434	14	135.0441	$C_8H_7O_2$	-5.18	
M12	*N*-Deethylation +	ESI +	PI at *m/z* 224.1272	2	224.1281	$C_{12}H_{18}O_3N$	-4.02	3.19

	reduction diastereomer 1		FI at *m/z* 206.1167	24	206.1176	$C_{12}H_{16}O_2N$	-4.37	
			FI at *m/z* 174.0906	100	174.0913	$C_{11}H_{12}ON$	-4.02	
			FI at *m/z* 151.0383	5	151.0390	$C_8H_7O_3$	-4.63	
			FI at *m/z* 146.0957	7	146.0964	$C_{10}H_{12}N$	-4.79	
			FI at *m/z* 72.0812	22	72.0808	$C_4H_{10}N$	5.55	
M13	*N*-Deethylation + reduction diastereomer 2	ESI +	PI at *m/z* 224.1270	2	224.1281	$C_{12}H_{18}O_3N$	-4.91	3.52
			FI at *m/z* 206.1165	25	206.1176	$C_{12}H_{16}O_2N$	-5.34	
			FI at *m/z* 174.0906	100	174.0913	$C_{11}H_{12}ON$	-4.02	
			FI at *m/z* 151.0384	5	151.0390	$C_8H_7O_3$	-3.97	
			FI at *m/z* 146.0957	7	146.0964	$C_{10}H_{12}N$	-4.79	
			FI at *m/z* 72.0812	23	72.0808	$C_4H_{10}N$	5.55	
M14	*N*-Deethylation + demethylenation + methylation isomer 2	ESI +	PI at *m/z* 224.1270	3	224.1281	$C_{12}H_{18}O_3N$	-4.91	3.83
			FI at *m/z* 206.1164	100	206.1176	$C_{12}H_{16}O_2N$	-5.82	
			FI at *m/z* 164.0698	39	164.0706	$C_9H_{10}O_2N$	-4.88	
			FI at *m/z* 150.0543	3	150.0550	$C_8H_8O_2N$	-4.66	
			FI at *m/z* 135.0434	12	135.0441	$C_8H_7O_2$	-5.18	
M15	Demethylenation	ESI +	PI at *m/z* 238.1433	59	238.1438	$C_{13}H_{20}O_3N$	-2.10	3.14
			FI at *m/z* 220.1330	100	220.1332	$C_{13}H_{18}O_2N$	-0.91	
			FI at *m/z* 202.1225	87	202.1226	$C_{13}H_{16}ON$	-0.49	
			FI at *m/z* 177.0782	34	177.0784	$C_{10}H_{11}O_2N$	-1.13	
			FI at *m/z* 123.0441	38	123.0441	$C_7H_7O_2$	0.00	
			FI at *m/z* 100.1125	32	100.1121	$C_6H_{14}N$	4.00	
M16	Demethylenation + methylation isomer 1	ESI +	PI at *m/z* 252.1591	40	252.1594	$C_{14}H_{22}O_3N$	-1.19	3.51
			FI at *m/z* 234.1484	63	234.1489	$C_{14}H_{20}O_2N$	-2.14	
			FI at *m/z* 202.1224	100	202.1226	$C_{13}H_{16}ON$	-0.99	
			FI at *m/z* 175.0751	30	175.0754	$C_{11}H_{11}O_2$	-1.71	
			FI at *m/z* 151.0389	11	151.0390	$C_8H_7O_3$	-0.66	
			FI at *m/z* 100.1125	62	100.1121	$C_6H_{14}N$	4.00	
M17	Demethylenation + methylation isomer 2	ESI +	PI at *m/z* 252.1589	40	252.1594	$C_{14}H_{22}O_3N$	-1.98	3.81
			FI at *m/z* 234.1486	61	234.1489	$C_{14}H_{20}O_2N$	-1.28	
			FI at *m/z* 202.1225	100	202.1226	$C_{13}H_{16}ON$	-0.49	
			FI at *m/z* 175.0752	32	175.0754	$C_{11}H_{11}O_2$	-1.14	
			FI at *m/z* 151.0390	12	151.0390	$C_8H_7O_3$	0.00	
			FI at *m/z* 100.1125	63	100.1121	$C_6H_{14}N$	4.00	
M18	Reduction diastereomer 1	ESI +	PI at *m/z* 252.1604	3	252.1594	$C_{14}H_{22}O_3N$	3.97	4.38
			FI at *m/z* 234.1484	100	234.1489	$C_{14}H_{20}O_2N$	-2.14	
			FI at *m/z* 191.0937	25	191.0935	$C_{11}H_{13}O_2N$	1.05	
			FI at *m/z* 149.0596	1	149.0597	$C_9H_9O_2$	-0.67	
			FI at *m/z* 98.0968	3	98.0964	$C_6H_{12}N$	4.08	
M19	Reduction diastereomer 2	ESI +	PI at *m/z* 252.1589	4	252.1594	$C_{14}H_{22}O_3N$	-1.98	4.50
			FI at *m/z* 234.1479	100	234.1489	$C_{14}H_{20}O_2N$	-4.27	
			FI at *m/z* 191.0932	25	191.0935	$C_{11}H_{13}O_2N$	-1.57	
			FI at *m/z* 149.0591	1	149.0597	$C_9H_9O_2$	-4.03	
			FI at *m/z* 98.0964	4	98.0964	$C_6H_{12}N$	0.00	
M20	Hydroxylation	ESI +	PI at *m/z* 266.1384	100	266.1387	$C_{14}H_{20}O_4N$	-1.13	3.68
			FI at *m/z* 248.1279	8	248.1281	$C_{14}H_{18}O_3N$	-0.81	
			FI at *m/z* 230.1176	31	230.1176	$C_{14}H_{16}O_2N$	0.00	
			FI at *m/z* 206.0810	84	206.0812	$C_{11}H_{12}O_3N$	-0.97	
			FI at *m/z* 176.0706	30	176.0706	$C_{10}H_{10}O_2N$	0.00	
			FI at *m/z* 72.0815	16	72.0808	$C_4H_{10}N$	9.71	
M21	*N*-Oxygenation	ESI +	PI at *m/z* 266.1383	8	266.1387	$C_{14}H_{20}O_4N$	-1.50	5.52
			FI at *m/z* 248.1274	2	248.1281	$C_{14}H_{18}O_3N$	-2.82	
			FI at *m/z* 176.0701	2	176.0706	$C_{10}H_{10}O_2N$	-2.84	
			FI at *m/z* 149.0233	100	149.0233	$C_8H_5O_3$	0.00	
			FI at *m/z* 121.0285	2	121.0284	$C_7H_5O_2$	0.83	
			FI at *m/z* 116.1072	7	116.1070	$C_6H_{14}ON$	1.72	
M22	Demethylenation + sulfation isomer 1	ESI +	PI at *m/z* 318.0999	54	318.1006	$C_{13}H_{20}O_6NS$	-2.20	3.19
			FI at *m/z* 238.1437	100	238.1438	$C_{13}H_{20}O_3N$	-0.42	
			FI at *m/z* 220.1333	94	220.1332	$C_{13}H_{18}O_2N$	0.45	
			FI at *m/z* 202.1224	95	202.1226	$C_{13}H_{16}ON$	-0.99	
			FI at *m/z* 123.0443	43	123.0441	$C_7H_7O_2$	1.63	

			FI at *m/z* 100.1126	9	100.1121	$C_6H_{14}N$	4.99	
M23	Demethylenation + sulfation isomer 2	ESI +	PI at *m/z* 318.1004	41	318.1006	$C_{13}H_{20}O_6NS$	-0.63	3.43
			FI at *m/z* 238.1438	89	238.1438	$C_{13}H_{20}O_3N$	0.00	
			FI at *m/z* 220.1333	100	220.1332	$C_{13}H_{18}O_2N$	0.45	
			FI at *m/z* 202.1225	65	202.1226	$C_{13}H_{16}ON$	-0.49	
			FI at *m/z* 123.0444	27	123.0441	$C_7H_7O_2$	2.44	
			FI at *m/z* 100.1124	25	100.1121	$C_6H_{14}N$	3.00	
M24	Demethylenation + methylation + sulfation	ESI +	PI at *m/z* 332.1154	15	332.1162	$C_{14}H_{22}O_6NS$	-2.41	3.55
			FI at *m/z* 252.1591	92	252.1594	$C_{14}H_{22}O_3N$	-1.19	
			FI at *m/z* 234.1486	66	234.1489	$C_{14}H_{20}O_2N$	-1.28	
			FI at *m/z* 202.1225	100	202.1226	$C_{13}H_{16}ON$	-0.49	
			FI at *m/z* 100.1125	56	100.1121	$C_6H_{14}N$	4.00	
M25	Demethylenation + glucuronidation isomer 1	ESI +	PI at *m/z* 414.1740	44	414.1759	$C_{19}H_{28}O_9N$	-4.59	1.95
			FI at *m/z* 238.1425	100	238.1438	$C_{13}H_{20}O_3N$	-5.46	
			FI at *m/z* 220.1320	88	220.1332	$C_{13}H_{18}O_2N$	-5.45	
			FI at *m/z* 202.1216	67	202.1226	$C_{13}H_{16}ON$	-4.95	
			FI at *m/z* 123.0437	28	123.0441	$C_7H_7O_2$	-3.25	
			FI at *m/z* 100.1121	24	100.1121	$C_6H_{14}N$	0.00	
M26	Demethylenation + glucuronidation isomer 2	ESI +	PI at *m/z* 414.1753	36	414.1759	$C_{19}H_{28}O_9N$	-1.45	2.92
			FI at *m/z* 238.1434	64	238.1438	$C_{13}H_{20}O_3N$	-1.68	
			FI at *m/z* 220.1330	100	220.1332	$C_{13}H_{18}O_2N$	-0.91	
			FI at *m/z* 202.1225	66	202.1226	$C_{13}H_{16}ON$	-0.49	
			FI at *m/z* 123.0440	27	123.0441	$C_7H_7O_2$	-0.81	
			FI at *m/z* 100.1125	56	100.1121	$C_6H_{14}N$	4.00	
M27	Demethylenation + methylation + glucuronidation isomer 1	ESI +	PI at *m/z* 428.1910	16	428.1915	$C_{20}H_{30}O_9N$	-1.17	2.80
			FI at *m/z* 252.1590	100	252.1594	$C_{14}H_{22}O_3N$	-1.59	
			FI at *m/z* 234.1485	60	234.1489	$C_{14}H_{20}O_2N$	-1.71	
			FI at *m/z* 202.1225	90	202.1226	$C_{13}H_{16}ON$	-0.99	
			FI at *m/z* 100.1125	58	100.1121	$C_6H_{14}N$	4.00	
M28	Demethylenation + methylation + glucuronidation isomer 2	ESI +	PI at *m/z* 428.1915	27	428.1915	$C_{20}H_{30}O_9N$	0.00	3.25
			FI at *m/z* 252.1591	98	252.1594	$C_{14}H_{22}O_3N$	-1.19	
			FI at *m/z* 234.1485	82	234.1489	$C_{14}H_{20}O_2N$	-1.71	
			FI at *m/z* 202.1224	100	202.1226	$C_{13}H_{16}ON$	-0.99	
			FI at *m/z* 100.1125	42	100.1121	$C_6H_{14}N$	4.00	
NEH (parent compound)	-	ESI +	PI at *m/z* 220.1691	40	220.1696	$C_{14}H_{22}ON$	-2.27	4.89
			FI at *m/z* 202.1587	100	202.1590	$C_{14}H_{20}N$	-1.48	
			FI at *m/z* 175.1116	18	175.1117	$C_{12}H_{15}O$	-0.57	
			FI at *m/z* 146.0962	73	146.0964	$C_{10}H_{12}N$	-1.37	
			FI at *m/z* 118.0653	44	118.0651	C_8H_8N	1.69	
			FI at *m/z* 91.0547	82	91.0542	C_7H_7	5.49	
M29	*N*-Deethylation	ESI +	PI at *m/z* 192.1380	4	192.1383	$C_{12}H_{18}ON$	-1.56	4.60
			FI at *m/z* 175.1116	20	175.1117	$C_{12}H_{15}O$	-0.57	
			FI at *m/z* 174.1275	57	174.1277	$C_{12}H_{16}N$	-1.15	
			FI at *m/z* 118.0653	100	118.0651	C_8H_8N	1.69	
			FI at *m/z* 91.0547	81	91.0542	C_7H_7	5.49	
M30	*N*-Deethylation + reduction	ESI +	PI at *m/z* 194.1540	3	194.1539	$C_{12}H_{20}ON$	0.52	4.46
			FI at *m/z* 176.1432	100	176.1434	$C_{12}H_{18}N$	-1.14	
			FI at *m/z* 120.0809	18	120.0808	$C_8H_{10}N$	0.83	
			FI at *m/z* 91.0547	33	91.0542	C_7H_7	5.49	
M31	Reduction	ESI +	PI at *m/z* 222.1851	5	222.1852	$C_{14}H_{24}ON$	-0.45	4.99
			FI at *m/z* 204.1745	100	204.1747	$C_{14}H_{20}N$	-0.98	
			FI at *m/z* 176.1432	2	176.1434	$C_{10}H_{13}N$	-1.14	
			FI at *m/z* 147.1040	13	147.1043	$C_{10}H_{13}N$	-2.04	
			FI at *m/z* 91.0547	14	91.0542	C_7H_7	5.49	
M32	*N*-Deethylation + *N*-acetylation	ESI +	PI at *m/z* 234.1496	2	234.1489	$C_{14}H_{20}O_2N$	2.99	6.45
			FI at *m/z* 192.1380	100	192.1383	$C_{12}H_{18}ON$	-1.56	
			FI at *m/z* 175.1117	60	175.1117	$C_{12}H_{15}O$	0.00	
			FI at *m/z* 174.1275	84	174.1277	$C_{12}H_{16}N$	-1.15	
			FI at *m/z* 118.0653	64	118.0651	C_8H_8N	1.69	
			FI at *m/z* 91.0547	67	91.0542	C_7H_7	5.49	
M33	Hydroxylation	ESI +	PI at *m/z* 236.1635	100	236.1645	$C_{14}H_{22}O_2N$	-4.23	3.70

	isomer 1		FI at *m/z* 218.1528	45	218.1539	$C_{14}H_{20}ON$	-5.04	
			FI at *m/z* 200.1425	20	200.1434	$C_{14}H_{18}N$	-4.50	
			FI at *m/z* 173.0954	38	173.0961	$C_{12}H_{13}O$	-4.04	
			FI at *m/z* 158.0958	88	158.0964	$C_{11}H_{12}N$	-3.80	
			FI at *m/z* 105.0334	12	105.0335	C_7H_5O	-0.95	
			FI at *m/z* 91.0544	30	91.0542	C_7H_7	2.20	
M34	Hydroxylation isomer 2	ESI +	PI at *m/z* 236.1649	27	236.1645	$C_{14}H_{22}O_2N$	1.69	4.23
			FI at *m/z* 218.1537	100	218.1539	$C_{14}H_{20}ON$	-0.92	
			FI at *m/z* 191.1065	16	191.1067	$C_{12}H_{15}O_2$	-1.05	
			FI at *m/z* 162.0912	38	162.0913	$C_{10}H_{12}ON$	-0.62	
			FI at *m/z* 107.0495	48	107.0491	C_7H_7O	3.74	
M35	Reduction + hydroxylation	ESI +	PI at *m/z* 238.1791	22	238.1802	$C_{14}H_{24}O_2N$	-4.62	3.54
			FI at *m/z* 220.1695	14	220.1696	$C_{14}H_{22}ON$	-0.45	
			FI at *m/z* 202.1581	8	202.1590	$C_{14}H_{20}N$	-4.45	
			FI at *m/z* 175.1109	31	175.1117	$C_{12}H_{15}O$	-4.57	
			FI at *m/z* 160.1114	8	160.1121	$C_{11}H_{14}N$	-4.37	
			FI at *m/z* 105.0339	1	105.0335	C_7H_5O	3.81	
			FI at *m/z* 91.0544	100	91.0542	C_7H_7	5.49	
M36	Carboxylation	ESI +	PI at *m/z* 250.1435	49	250.1438	$C_{14}H_{20}O_3N$	-1.20	3.59
			FI at *m/z* 232.1332	15	232.1332	$C_{14}H_{18}O_2N$	0.00	
			FI at *m/z* 214.1227	16	214.1226	$C_{14}H_{16}ON$	0.47	
			FI at *m/z* 202.1229	2	202.1226	$C_{13}H_{16}ON$	1.48	
			FI at *m/z* 158.1176	19	158.1176	$C_8H_{16}O_2N$	0.00	
			FI at *m/z* 91.0544	100	91.0542	C_7H_7	2.20	
M37	Reduction + glucuronidation diastereomer 1	ESI +	PI at *m/z* 398.2171	18	398.2173	$C_{20}H_{32}O_7N$	-0.50	4.61
			FI at *m/z* 222.1848	10	222.1852	$C_{14}H_{24}ON$	-1.80	
			FI at *m/z* 204.1744	100	204.1747	$C_{14}H_{20}N$	-1.47	
			FI at *m/z* 147.1040	13	147.1043	$C_{10}H_{13}N$	-2.04	
			FI at *m/z* 91.0547	9	91.0542	C_7H_7	5.49	
M38	Reduction + glucuronidation diastereomer 2	ESI +	PI at *m/z* 398.2165	23	398.2173	$C_{20}H_{32}O_7N$	-2.01	4.86
			FI at *m/z* 222.1855	4	222.1852	$C_{14}H_{24}ON$	1.35	
			FI at *m/z* 204.1745	100	204.1747	$C_{14}H_{20}N$	-0.98	
			FI at *m/z* 147.1042	14	147.1043	$C_{10}H_{13}N$	-0.68	
			FI at *m/z* 91.0548	11	91.0542	C_7H_7	6.59	
M39	Hydroxylation + glucuronidation isomer 1	ESI +	PI at *m/z* 412.1969	25	412.1966	$C_{20}H_{30}O_8N$	0.73	3.03
			FI at *m/z* 236.1642	76	236.1645	$C_{14}H_{22}O_2N$	-1.27	
			FI at *m/z* 218.1536	100	218.1539	$C_{14}H_{20}ON$	-1.38	
			FI at *m/z* 191.1064	7	191.1067	$C_{12}H_{15}O_2$	-1.57	
			FI at *m/z* 162.0912	22	162.0913	$C_{10}H_{12}ON$	-0.62	
			FI at *m/z* 107.0495	39	107.0491	C_7H_7O	3.74	
M40	Hydroxylation + glucuronidation isomer 2	ESI +	PI at *m/z* 412.1949	17	412.1966	$C_{20}H_{30}O_8N$	-4.12	3.51
			FI at *m/z* 236.1633	100	236.1645	$C_{14}H_{22}O_2N$	-5.08	
			FI at *m/z* 218.1530	52	218.1539	$C_{14}H_{20}ON$	-4.13	
			FI at *m/z* 200.1425	6	200.1434	$C_{14}H_{18}N$	-4.50	
			FI at *m/z* 173.0957	4	173.0961	$C_{12}H_{13}O$	-2.31	
			FI at *m/z* 158.0958	25	158.0964	$C_{11}H_{12}N$	-3.80	
			FI at *m/z* 105.0336	4	105.0335	C_7H_5O	0.95	
			FI at *m/z* 91.0545	8	91.0542	C_7H_7	3.29	
4F-PHP (parent compound)	-	ESI +	PI at *m/z* 264.1755	100	264.1758	$C_{16}H_{23}ONF$	-1.14	5.09
			FI at *m/z* 193.1021	12	193.1023	$C_{12}H_{14}OF$	-1.04	
			FI at *m/z* 140.1432	31	140.1434	$C_9H_{18}N$	-1.43	
			FI at *m/z* 123.0242	16	123.0241	C_7H_4OF	0.81	
			FI at *m/z* 109.0451	73	109.0448	C_7H_6F	2.75	
			FI at *m/z* 72.0815	4	72.0808	C_4H_8N	9.71	
M41	*N*,*N*-Dealkylation	ESI+	PI at *m/z* 210.1291	6	210.1289	$C_{12}H_{17}ONF$	0.95	4.74
			FI at *m/z* 193.1022	23	193.1023	$C_{12}H_{14}OF$	-0.52	
			FI at *m/z* 192.1180	93	192.1183	$C_{12}H_{15}NF$	-1.56	
			FI at *m/z* 136.0556	100	136.0557	C_8H_7NF	-0.73	
			FI at *m/z* 123.0242	16	123.0241	C_7H_4OF	0.81	
			FI at *m/z* 109.0451	91	109.0448	C_7H_6F	2.75	
M42	Reduction	ESI +	PI at *m/z* 266.1910	29	266.1915	$C_{16}H_{25}ONF$	-1.88	5.29

			FI at *m/z* 248.1807	100	248.1809	$C_{16}H_{23}NF$	-0.81	
			FI at *m/z* 191.1103	46	191.1105	$C_{12}H_{14}NF$	-1.05	
			FI at *m/z* 109.0451	9	109.0448	C_7H_6F	2.75	
			FI at *m/z* 72.0815	10	72.0808	$C_4H_{10}N$	9.71	
M43	Carbonylation isomer 1	ESI +	PI at *m/z* 278.1538	8	278.1551	$C_{16}H_{21}O_2NF$	-4.67	4.87
			FI at *m/z* 193.1014	33	193.1023	$C_{12}H_{14}OF$	-4.66	
			FI at *m/z* 123.0237	1	123.0241	C_7H_4OF	-3.25	
			FI at *m/z* 109.0447	100	109.0448	C_7H_6F	-0.92	
			FI at *m/z* 86.0602	23	86.0600	C_4H_8ON	2.32	
M44	Carbonylation isomer 2	ESI +	PI at *m/z* 278.1539	62	278.1551	$C_{16}H_{21}O_2NF$	-4.31	7.33
			FI at *m/z* 193.1015	29	193.1023	$C_{12}H_{14}OF$	-4.14	
			FI at *m/z* 154.1218	15	154.1226	$C_9H_{16}ON$	-5.19	
			FI at *m/z* 123.0237	7	123.0241	C_7H_4OF	-3.25	
			FI at *m/z* 109.0447	100	109.0448	C_7H_6F	-0.92	
			FI at *m/z* 86.0603	29	86.0600	C_4H_8ON	3.49	
M45	Hydroxylation isomer 1	ESI +	PI at *m/z* 280.1695	100	280.1707	$C_{16}H_{23}O_2NF$	-4.28	3.84
			FI at *m/z* 262.1592	22	262.1602	$C_{16}H_{21}ONF$	-3.81	
			FI at *m/z* 204.1174	38	204.1183	$C_{13}H_{15}NF$	-4.41	
			FI at *m/z* 191.0857	2	191.0867	$C_{12}H_{12}OF$	-5.23	
			FI at *m/z* 156.1377	2	156.1383	$C_9H_{18}ON$	-3.84	
			FI at *m/z* 123.0237	7	123.0241	C_7H_4OF	-3-25	
			FI at *m/z* 109.0446	17	109.0448	C_7H_6F	-1.83	
			FI at *m/z* 72.0812	19	72.0808	$C_4H_{10}N$	5.55	
M46	Hydroxylation isomer 2	ESI +	PI at *m/z* 280.1693	100	280.1707	$C_{16}H_{23}O_2NF$	-5.00	3.95
			FI at *m/z* 262.1588	15	262.1602	$C_{16}H_{21}ONF$	-5.34	
			FI at *m/z* 204.1172	5	204.1183	$C_{13}H_{15}NF$	-5.39	
			FI at *m/z* 191.0860	2	191.0867	$C_{12}H_{12}OF$	-3.66	
			FI at *m/z* 156.1376	4	156.1383	$C_9H_{18}ON$	-4.48	
			FI at *m/z* 123.0236	3	123.0241	C_7H_4OF	-4.06	
			FI at *m/z* 109.0447	14	109.0448	C_7H_6F	-0.92	
			FI at *m/z* 72.0812	22	72.0808	$C_4H_{10}N$	5.55	
M47	Hydroxylation isomer 3	ESI +	PI at *m/z* 280.1703	100	280.1707	$C_{16}H_{23}O_2NF$	-1.43	4.89
			FI at *m/z* 262.1599	8	262.1602	$C_{16}H_{21}ONF$	-1.14	
			FI at *m/z* 234.1653	3	234.1653	$C_{15}H_{21}NF$	0.00	
			FI at *m/z* 193.1022	10	193.1023	$C_{12}H_{14}OF$	-0.52	
			FI at *m/z* 156.1382	18	156.1383	$C_9H_{18}ON$	-0.64	
			FI at *m/z* 123.0242	38	123.0241	C_7H_4OF	0.81	
			FI at *m/z* 109.0451	67	109.0448	C_7H_6F	2.75	
			FI at *m/z* 70.0659	13	70.0651	C_4H_8N	11.42	
M48	Reduction + glucuronidation diastereomer 1	ESI +	PI at *m/z* 442.2214	21	442.2236	$C_{22}H_{33}O_7NF$	-4.97	4.88
			FI at *m/z* 266.1902	4	266.1915	$C_{16}H_{25}ONF$	-4.88	
			FI at *m/z* 248.1797	100	248.1809	$C_{16}H_{23}NF$	-4.84	
			FI at *m/z* 191.1094	59	191.1105	$C_{12}H_{14}NF$	-5.76	
			FI at *m/z* 109.0446	9	109.0448	C_7H_6F	-1.83	
			FI at *m/z* 72.0813	3	72.0808	$C_4H_{10}N$	6.94	
M49	Reduction + glucuronidation diastereomer 2	ESI +	PI at *m/z* 442.2217	34	442.2236	$C_{22}H_{33}O_7NF$	-4.30	5.04
			FI at *m/z* 266.1904	5	266.1915	$C_{16}H_{25}ONF$	-4.13	
			FI at *m/z* 248.1795	100	248.1809	$C_{16}H_{23}NF$	-5.64	
			FI at *m/z* 191.1095	61	191.1105	$C_{12}H_{14}NF$	-5.23	
			FI at *m/z* 109.0446	10	109.0448	C_7H_6F	-1.83	
			FI at *m/z* 72.0812	9	72.0808	$C_4H_{10}N$	5.55	
M50	Hydroxylation + glucuronidation isomer 1	ESI +	PI at *m/z* 456.2007	30	456.2028	$C_{22}H_{31}O_8NF$	-4.60	3.78
			FI at *m/z* 280.1698	100	280.1707	$C_{16}H_{23}O_2NF$	-3.21	
			FI at *m/z* 262.1594	18	262.1602	$C_{16}H_{21}ONF$	-3.05	
			FI at *m/z* 204.1179	4	204.1183	$C_{13}H_{15}NF$	-1.96	
			FI at *m/z* 191.0858	1	191.0867	$C_{12}H_{12}OF$	-4.71	
			FI at *m/z* 123.0236	4	123.0241	C_7H_4OF	-4.06	
			FI at *m/z* 109.0448	11	109.0448	C_7H_6F	0.00	
			FI at *m/z* 72.0812	22	72.0808	$C_4H_{10}N$	5.55	
M51	Hydroxylation + glucuronidation	ESI +	PI at *m/z* 456.2019	81	456.2028	$C_{22}H_{31}O_8NF$	-1.97	4.57
			FI at *m/z* 280.1704	100	280.1707	$C_{16}H_{23}O_2NF$	-1.07	

	isomer 2		FI at *m/z* 262.1601	23	262.1602	$C_{16}H_{21}ONF$	-0.38	
			FI at *m/z* 234.1663	4	234.1653	$C_{15}H_{21}NF$	4.27	
			FI at *m/z* 193.1030	11	193.1023	$C_{12}H_{14}OF$	3.63	
			FI at *m/z* 156.1382	6	156.1383	$C_{9}H_{18}ON$	-0.64	
			FI at *m/z* 123.0242	76	123.0241	$C_{7}H_{4}OF$	0.81	
			FI at *m/z* 109.0452	75	109.0448	$C_{7}H_{6}F$	3.67	
			FI at *m/z* 70.0658	26	70.0651	$C_{4}H_{8}N$	9.99	

Table S2. Absolute peak areas of 4-CEC, ephylone, NEH, 4F-PHP, and their phase I and II metabolites in MS^1 (ESI +) derived from analyses of authentic human biosamples and pS9 incubations by LC-HRMS/MS. Plasma sample was diluted 1:4 and urine sample concentrated 1:2 during sample preparation. The three largest peak areas of each compound and matrix are given in bold. Metabolites IDs correspond to Table S1. n.d., not detected

Metabolite ID	Metabolic reaction	Human biosamples		pS9 incubations	
		Plasma	Urine	1 hour	6 hours
4-CEC (parent compound)	-	**1.28E+06**	**4.83E+08**	**3.30E+09**	**1.77E+09**
M1	*N*-Deethylation	5.30E+05	1.85E+07	**1.61E+07**	**2.21E+07**
M2	*N*-Deethylation + reduction	**1.10E+06**	**5.67E+08**	1.06E+05	4.30E+05
M3	Reduction	**3.61E+07**	**3.43E+09**	**2.45E+08**	**1.66E+08**
M4	*N*-Oxygenation	n.d.	n.d.	1.28E+07	1.19E+07
M5	Carboxylation	n.d.	2.38E+06	n.d.	n.d.
M6	*N*-Deethylation + malonylation	n.d.	1.63E+06	n.d.	n.d.
M7	*N*-Deethylation + succinylation	n.d.	1.86E+08	n.d.	n.d.
M8	*N*-Deethylation + glutarylation	n.d.	1.64E+07	n.d.	n.d.
M9	Reduction + glucuronidation	8.58E+04	1.47E+08	n.d.	n.d.
Ephylone (parent compound)	-	**7.37E+06**	**8.35E+08**	**6.91E+09**	**3.98E+09**
M10	*N*-Deethylation	8.83E+05	7.50E+07	3.25E+07	4.97E+07
M11	*N*-Deethylation + demethylenation + methylation isomer 1	n.d.	3.48E+07	n.d.	n.d.
M12	*N*-Deethylation + reduction diastereomer 1	n.d.	8.46E+07	n.d.	n.d.
M13	*N*-Deethylation + reduction diastereomer 2	n.d.	2.52E+07	n.d.	n.d.
M14	*N*-Deethylation + demethylenation + methylation isomer 2	n.d.	3.07E+07	n.d.	n.d.
M15	Demethylenation	5.65E+05	8.10E+07	2.25E+07	1.09E+07
M16	Demethylenation + methylation isomer 1	6.07E+05	2.42E+08	2.85E+07	**2.43E+08**
M17	Demethylenation + methylation isomer 2	1.82E+05	7.24E+07	**1.26E+08**	**8.07E+07**
M18	Reduction diastereomer 1	3.18E+05	5.69E+07	**4.90E+07**	2.87E+07
M19	Reduction	n.d.	6.56E+07	n.d.	n.d.

	diastereomer 2				
M20	Hydroxylation	n.d.	3.68E+06	4.84E+05	1.18E+06
M21	*N*-Oxygenation	n.d.	n.d.	7.84E+06	8.06E+06
M22	Demethylenation + sulfation isomer 1	n.d.	4.94E+06	4.01E+05	9.27E+05
M23	Demethylenation + sulfation isomer 2	n.d.	4.38E+06	3.68E+05	8.81E+05
M24	Demethylenation + methylation + sulfation	n.d.	1.07E+07	4.71E+06	1.58E+07
M25	Demethylenation + glucuronidation isomer 1	n.d.	1.09E+07	n.d.	n.d.
M26	Demethylenation + glucuronidation isomer 2	**2.47E+06**	**2.98E+08**	3.10E+06	2.05E+06
M27	Demethylenation + methylation + glucuronidation isomer 1	**1.46E+06**	**2.46E+08**	1.90E+07	4.04E+07
M28	Demethylenation + methylation + glucuronidation isomer 2	8.15E+05	1.76E+08	1.06E+07	1.12E+07
NEH (parent compound)	-	**8.86E+05**	**1.16E+08**	**4.45E+09**	**2.29E +09**
M29	*N*-Deethylation	**7.71E+05**	**7.29E+07**	**1.74E+08**	**2.40E+08**
M30	*N*-Deethylation + reduction	6.17E+05	6.18E+07	1.33E+07	9.38E+06
M31	Reduction	1.65E+05	5.28E+07	**2.23E+08**	**1.33E+08**
M32	*N*-Deethylation + *N*-acetylation	n.d.	n.d.	1.36E+06	1.31E+06
M33	Hydroxylation isomer 1	**6.56E+05**	**2.02E+08**	4.61E+07	6.79E+07
M34	Hydroxylation isomer 2	n.d.	3.83E+06	9.25E+06	8.33E+06
M35	Reduction + hydroxylation	n.d.	3.10E+07	n.d.	n.d.
M36	Carboxylation	n.d.	3.91E+07	n.d.	3.23E+05
M37	Reduction + glucuronidation diastereomer 1	n.d.	3.54E+07	n.d.	1.27E+05
M38	Reduction + glucuronidation diastereomer 2	n.d.	2.59E+07	n.d.	2.67E+04
M39	Hydroxylation + glucuronidation isomer 1	n.d.	1.43E+06	n.d.	3.53E+05
M40	Hydroxylation + glucuronidation isomer 2	n.d.	5.20E+06	n.d.	n.d.
4F-PHP (parent compound)	-	**1.16E+06**	5.41E+07	**7.47E+09**	**4.71E+09**
M41	*N*-Dealkylation	n.d.	3.05E+06	4.11E+06	5.01E+06
M42	Reduction	**3.23E+06**	4.17E+07	**6.55E+08**	**4.92E+08**

M43	Carbonylation isomer 1	**9.62E+05**	**7.29E+07**	n.d.	n.d.
M44	Carbonylation isomer 2	2.76E+05	**6.68E+07**	5.15E+07	5.10E+07
M45	Hydroxylation isomer 1	n.d.	4.45E+06	8.01E+06	1.59E+07
M46	Hydroxylation isomer 2	n.d.	6.53E+06	5.66E+06	1.08E+07
M47	Hydroxylation isomer 3	n.d.	n.d.	**6.78E+07**	**1.11E+08**
M48	Reduction + glucuronidation diastereomer 1	n.d.	7.57E+06	n.d.	n.d.
M49	Reduction + glucuronidation diastereomer 2	n.d.	**8.71E+07**	2.08E+05	3.12E+05
M50	Hydroxylation + glucuronidation isomer 1	n.d.	2.79E+06	n.d.	n.d.
M51	Hydroxylation + glucuronidation isomer 2	n.d.	1.51E+07	8.17E+05	1.93E+06

Table S3. Targets identified in authentic human urine by means of GC-MS. Metabolites IDs correspond to Table S1. AC, acetylated

Metabolite ID	Target	Precursor ion mass, *m/z*	Fragment ion masses, *m/z*	Retention index
Parent compound	4-CEC AC	253	72, 111, 114, 139	1920
M2	*N*-Deethyl dihydro 4-CEC 2AC	269	72, 111, 114, 141	1995
M3	Dihydro 4-CEC 2AC	297	86, 111, 141	2100
Parent compound	Ephylone AC	291	100, 121, 142, 149	2275
M11/14	*N*-Deethyl-demethylenyl-methyl ephylone AC	265	72, 114, 151	2230
M11/14	*N*-Deethyl-demethylenyl-methyl ephylone 2AC	307	72, 114, 151, 193, 265	2300
M16/17	Demethylenyl-methyl ephylone AC	293	100, 123, 142, 151	2265
M16/17	Demethylenyl-methyl ephylone isomer 1 2AC	335	100, 123, 142, 151	2355
M16/17	Demethylenyl-methyl ephylone isomer 2 2AC	335	100, 123, 142, 151	2395
Parent compound	NEH AC	261	77, 105, 114, 156	2030